Institute for Molecular Medicine Finland (FIMM)
Helsinki Institute of Life Science, Doctoral School in Health Sciences,
Doctoral Programme in Integrative Life Sciences,
University of Helsinki

THE NUP98-NSD1 FUSION GENE IN ACUTE MYELOID LEUKEMIA

Jarno Kivioja

ACADEMIC DISSERTATION

To be presented, with the permission of the Faculty of Biological and Environmental Sciences, University of Helsinki, for public examination in lecture hall 2, Haartmaninkatu 8, Helsinki on May 31st 2019 at 12 noon.

Helsinki 2019

Supervisors

Caroline Heckman, Ph.D.
Institute for Molecular Medicine Finland
Helsinki Institute of Life Science
University of Helsinki
Helsinki, Finland

Professor Kimmo Porkka, M.D., Ph.D.
Hematology Research Unit Helsinki
University of Helsinki and Helsinki University Hospital Comprehensive Cancer Center
Department of Hematology
Helsinki, Finland

Reviewers

Docent Mervi Taskinen, M.D., Ph.D.
Pediatric Research Center
Helsinki University Hospital
Helsinki, Finland

Adjunct Professor Jorrit Enserink, Ph.D.
Department of Molecular Cell Biology
Institute for Cancer Research
The Norwegian Radium Hospital
Oslo, Norway

Opponent

Associate Professor, Linda Fogelstrand, M.D., Ph.D.
Institute of Biomedicine, Department of Clinical Chemistry and Transfusion Medicine
Sahlgrenska University Hospital
Gothenburg, Sweden

ISBN 978-951-51-5128-5 (paperback)
ISBN 978-951-51-5129-2 (PDF)
Unigrafia
Helsinki 2019

TABLE OF CONTENTS

ORIGINAL ARTICLES

This thesis is based on the following two research articles, which are referred to in the text by their roman numerals:

I: Kivioja JL, Lopez Martí JM, Kumar A, Kontro M, Edgren H, Parsons A, Lundán T, Wolf M, Porkka K, Heckman CA (2018). Chimeric *NUP98-NSD1* transcripts from the cryptic t(5;11)(q35;p15.4) in adult de novo acute myeloid leukemia. *Leukemia & Lymphoma*. 2018 Mar; 59 (3): 725-732.

II: Kivioja JL, Thanasopoulou A, Kumar A, Kontro M, Yadav B, Majumder MM, Javarappa KK, Eldfors S, Schwaller J, Porkka K, Heckman CA. Dasatinib and navitoclax act synergistically to target *NUP98-NSD1*$^{+}$/*FLT3*-ITD^{+} acute myeloid leukemia. *Leukemia.* 2018 Dec 19. doi: 10.1038/s41375-018-0327-2. (Epub ahead of print)

ABBREVIATIONS

ALL	Acute lymphoblastic leukemia
Allo-HCT	Allogeneic hematopoietic cell transplant
AML	Acute myeloid leukemia
APL	Acute promyelocytic leukemia
BCL-2	B-cell lymphoma-2
BM	Bone marrow
CFP	Cerulean fluorescent protein
CGH	Comparative genomic hybridization
CML	Chronic myeloid leukemia
CN-AML	Cytogenetically normal AML
COG	Children's Oncology Group
CPM	Counts per million reads
CR	Complete remission
del	Deletion
DMSO	Dimethylsulfoxide
DNA	Deoxyribonucleic acid
DSRT	Drug sensitivity and resistance testing
DSS	Drug sensitivity score
EC_{50}	Half-maximal effective concentration
ELN	European LeukemiaNet
EMA	European medicines agency
EMD	Extramedullary disease
FAB	The French-American-British classification system
FDA	Food and drug administration
FG	Phenylalanine Glycine
FISH	Fluorescence in situ hybridization
FLT3	Fms-like tyrosine kinase 3
GFP	Green Fluorescent Protein
GO	Gemtuzumab ozogamicin
HDAC	Histone deacetylase
HMT	Histone methyltransferase
HOX	Homeobox
HPC	Hematopoietic progenitor cell
HSC	Hematopoietic stem cell
HSP90	Heat shock protein 90
IC_{50}	Half-maximal inhibitory concentration

Inv	inversion
ITD	Internal tandem duplication
LB	Luria broth
LSC	Leukemic stem cell
MAPK	Mitogen activated protein kinase
MDS	Myelodysplastic syndrome
MEK	Mitogen activated protein kinase kinase
MNC	Mononuclear cell
MLL	Mixed lineage leukemia
MRD	Minimal residual disease
MTOR	Mammalian target of rapamycin kinase
NCBI	National Center for Biotechnology Information
NCCN	National Comprehensive Cancer Network
NGS	Next-generation sequencing
NSD1	Nuclear receptor binding SET-domain protein 1
NUP98	Nucleoporin 98
OS	Overall survival
p	Short arm of chromosome
PCR	Polymerase chain reaction
q	Long arm of chromosome
RNA	Ribonucleic acid
SET	Su(var)3-9, Enhancer of zeste and Trithorax
t	Translocation
t-AML	Therapy-related AML
TCGA	The Cancer Genome Atlas
TKI	Tyrosine kinase inhibitor
WBC	White blood cell
WHO	The World health organization
WT1	Wilm’s tumour 1

ABSTRACT

The objective of this thesis was to facilitate molecular detection and treatment of acute myeloid leukemia (AML) patients with recurrent t(5;11)(q35;p15.4) translocation, which joins nucleoporin 98 (*NUP98*) and nuclear receptor binding SET-domain protein 1 (*NSD1*) genes together. These patients suffer from a malignant disease with highly unfavorable prognosis and no evidence regarding efficient therapeutic options.

In study I, we investigated *NUP98-NSD1* transcript variants from AML patients with t(5;11) to facilitate its molecular detection from newly diagnosed AML patients and from post-treatment samples. We focused on this topic since, comparably to many AML-defining translocations, the detection of t(5;11) relies on accurate molecular screening methods. This translocation cannot be captured using conventional cytogenetics (G-banding) due to its subtelomeric localization and small size. Moreover, potential for alternative fusion transcripts may further complicate detection of *NUP98-NSD1*. In this study, we discovered three chimeric *NUP98-NSD1* transcripts from an index patient, which were later validated from two additional patients. The transcripts harbored two alternative fusion junctions joining *NUP98* exon 11 or exon 12 to *NSD1* exon 6, alternative 5' donor site of *NUP98* exon 7, and skipping of *NSD1* exon 7. Intriguingly, relative frequency of the previously unknown fusion gene between *NUP98* exon 11 and *NSD1* exon 6 was found to increase in two patients during disease progression.

In study II, our aim was to identify novel, more efficient, and less toxic small-molecule inhibitors for the treatment of *NUP98-NSD1*$^{+}$ AML using high-throughput drug sensitivity and resistance testing together with RNA sequencing. By screening over 300 anti-cancer drugs on patient cells and experimentally generated mouse cell models, we found that multikinase inhibitor dasatinib and pan-BCL-2 inhibitor navitoclax effectively and specifically target BM MNCs expressing *NUP98-NSD1* and *FLT3*-ITD. In combinatorial drug screens, strong synergistic interactions were found between dasatinib and navitoclax. Gene expression analysis revealed up-regulation of genes encoding for targets of dasatinib and navitoclax, *LCK*, *FGR*, and *BCL2A1*. Furthermore, we discovered that *NUP98-NSD1*$^{+}$/*FLT3*-ITD^{+} BM MNCs are highly resistant to topoisomerase II inhibitors such as mitoxantrone. It remains to be investigated whether replacing

topoisomerase II inhibitors with dasatinib and navitoclax in AML induction therapy could lead to improvements in long-term survival in patients with *NUP98-NSD1* and concomitant *FLT3*-ITD.

1 INTRODUCTION

Acute myeloid leukemia (AML) has the worst survival rate of adult leukemias and remains among the most lethal cancers worldwide (1). The aggressive nature of AML results from a runaway proliferation of undifferentiated myeloid stem cells in the bone marrow (BM), which obstructs normal hematopoiesis. AML is generally a disease of elderly affecting mostly individuals of sixty-five years of age and older. In older patients (> 60 years), the 5-year overall survival (OS) rate is 10%, while it is roughly 40% in younger AML patients (< 60 years) (2). Due to population ageing, incidence of AML is expected to rise in Finland in the future.

The first cancer genome was sequenced in 2008 from a patient with AML (3) and since then, the AML-defining genomic and transcriptomic alterations have been comprehensively characterized (4, 5). Technological advances have shifted the bottleneck hindering development of more efficient drugs from lack of genomic information to current inefficiencies in translating the excessive information into useful diagnostic and prognostic biomarkers, predicting treatment responses, and developing molecularly targeted therapies. Translational challenges related to drug development cover variety of factors such as limitations of preclinical drug screening methods, undruggable mutations, and unfeasibility to develop drugs against infrequent alterations (6). Regardless of the hindrances, many exciting discoveries have shed light on the remarkable potential of personalized genomic medicine. The best-known examples of successfully designed targeted therapies against oncogenic fusion genes include imatinib for chronic myeloid leukemia (CML) with *BCR-ABL1* (7), all-*trans* retinoic acid for acute promyeloid leukemia (APL) with *PML-RARA* (8), and crizotinib for non-small cell carcinoma with *EML4-ALK* fusion gene (9).

While approximately 300 gene fusions are known in AML (10), only few of them have been functionally characterized and investigated as therapeutic targets. To tackle this challenge, we centered our attention on high-risk *NUP98-NSD1* fusion, which results from t(5;11)(q35;p15.4) translocation. This translocation is undetectable with traditional chromosome banding due to its cryptic nature and subtelomeric localization. An earlier study performed on myelodysplastic syndrome (MDS) patient with t(5;11) had detected two alternative *NUP98-NSD1* transcripts indicating that alternative transcripts exist and complicate molecular

monitoring of the fusion gene (11). To address this issue, we investigated whether novel *NUP98-NSD1* variants could be found in AML. The objective of study I was to ensure that presence of t(5;11) is accurately captured from newly diagnosed AML patients and during minimal residual disease (MRD) monitoring. In study II, we investigated NUP98-NSD1 as a potential target for therapeutic modulation, since these patients are notoriously chemoresistant and lack adequate medical treatment options.

In this thesis, we show evidence that RNA sequencing (RNA-Seq) is a powerful method for identifying novel fusion transcripts and gene expression changes that may be followed-up by targeted molecular screening methods. We also demonstrate that drug sensitivity and resistance testing (DSRT) assay is a sensitive preclinical screening assay for identifying molecularly specific drug responses for patients with recurrent fusion genes such as *NUP98-NSD1*.

2 REVIEW OF THE LITERATURE

2.1 Acute myeloid leukemia (AML)

The first publication regarding AML appeared in 1827 when a French surgeon named Alfred-Armand-Louis-Marie Velpeau reported his findings regarding an elderly man with fever, urinary stones, weakness, and enlarged liver and spleen (12). Along with these pathological features, the patient's blood appeared as porridge-like, filled with white corpuscles. Some years later, the condition was named ”leucocythemia” by J.H. Bennett who discovered differences in color and composition of blood between patients (13). In 1856 Rudolf Virchow detected abnormally high levels of leukocytes from a patient's blood using light microscopy and introduced the term ”leukemia”, which evolved from Greek word leukós (light in color, white) (14). Tracing the footsteps of earlier pioneers, Franz Neumann uncovered that leucocytes are made in the BM and introduced the term ”myeloid” in accordance with the Greek word muelós (marrow). Another key discovery of the 19th century was made by Wilhelm Ebstein who noticed that myeloid leukemias can progress either slowly or fast and thereby suggested the term ”acute leukemia” for rapidly progressing leukemias (15).

These early pioneers established a foundation to the whats, whys and wherefores of AML. Namely, to disease in which the ability of BM to replenish pools of differentiated hematopoietic cells has been stripped away by immature, yet exponentatially dividing leukemic cells. Consequently, the number of erythrocytes, platelets, neutrophils, and mature leucocytes plummet leading to chaotic stem-cell landscape and eventual BM failure. The lack of terminally differentiated cells (Figure 1) lead to various complications including fatigue, loss of apetite, infections, bruising, fever, blood clotting problems, and anemia (16). Although the malignant flock of descendants mainly accumulate in BM and blood, extramedullary disease (EMD) is found from roughly 25% of patients (17). EMD is most regularly present in patients with monocytic/myelomonocytic leukemia and in patients with high WBC counts (18). The most commonly infiltrated sites are lymph nodes, spleen, lungs, liver, skin, testicles, gingiva, and central nervous system, but PET/CT scans have identified as many as 55 distinct EMD sites. EMD is associated with lower CR and OS rates in AML (19).

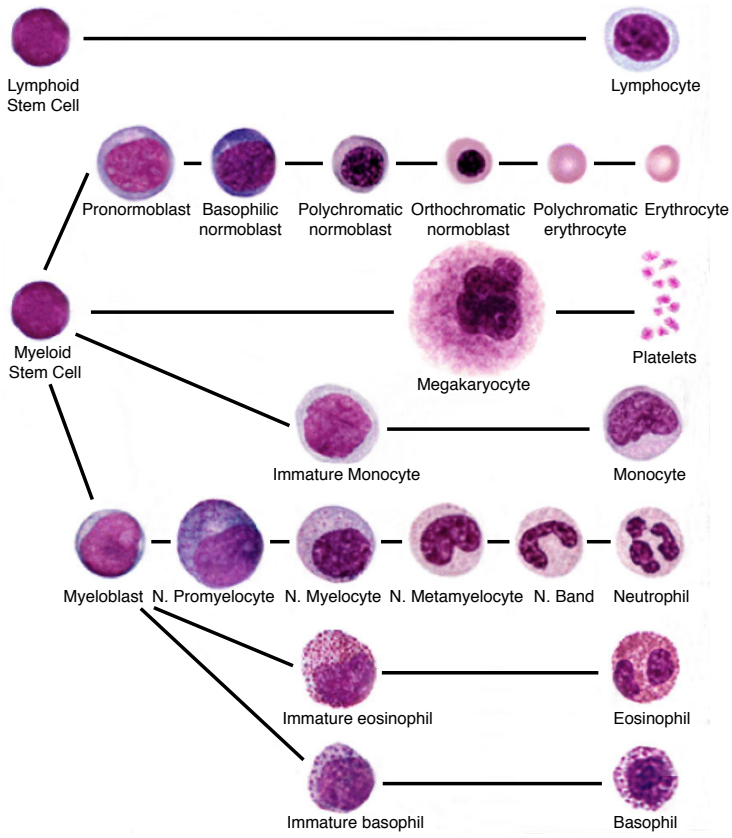

Figure 1 Maturation of blood cells. The schematic drawing shows morphological features of various hematopoietic cells of myeloid origin at different stages of maturation. In AML, the terminal differentiation is ceased by various genomic alterations that occur in multipotent HSCs or in the committed myeloid progenitors. *Adapted from online source* ***(20)***

2.1.1 Etiology

The exact etiology of how mutations arise and lead to AML remain elusive although many known and suspected risk factors exist. Associated risk factors include cigarette smoking (21), exposure to diesel and gasoline, glues, adhesives, paints, inks, pigments, pesticides and fertilizers, formaldehyde, chloramphenicol, radiation, and exposure to electric and magnetic field (22-25). Previous anti-cancer therapies have also been associated with increased likelihood of therapy-related AML (t-AML). The specific cancer treatments that may lead to AML-

causing mutations include type II topoisomerase inhibitors, alkylating agents, radioimmunotherapy, radiotherapy or their combination (26, 27). In a Danish study, 6.6% (203/3055) of AMLs were shown to have originated from previous anti-cancer therapy (28). True incidence of t-AML may be closer to 10% based on other studies (29).

Aside from environmental risk factors, AML may develop from inherited genetic alterations. Germline alterations occasionally predispose individuals to various hematological malignancies that later progress to AML. Up to now, at least 13 genetic diseases are known to occasionally develop into AML and include diseases such as Fanconi Anemia, Dyskeratosis congenita, Diamond Blackfan anemia, Li Fraumeni, Bloom syndrome, and Schwachman Diamond Syndrome (30). Wartiovaara-Kautto *et al* uncovered 34 germline variants from 16 genes that may predispose individuals to AML by exploring inherited mutations from 68 patients (31). Interestingly, 13% (8/62) of those AML patients had a close relative with a hematological disease. The list of most well-known predisposing germline variants include mutations in *ASXL1* (32), *DDX41* (33), *CEBPA* (34), *GATA2* (35), *RUNX1* (36), *TP53* (37), and trisomy 21 (38). Moreover, many other germline variants have been discovered from patients with AML and leukemia-associated predisposition syndromes. Interestingly, percentage of inherited AML may be lower in children than in adults. In a recent study, inherited mutations were found from 13 genes of 4% of pediatric AML patients (n = 588) (39).

Researchers have spent vast amount of time trying to reliably define the cell of origin in AML to generate knowledge about disease etiology and to facilitate the development of more efficient treatments. Current consensus is that AML arises as a result of multistep process (Figure 2). Mutations are acquired in the hematopoietic stem cells (HSCs) and hematopoietic progenitor cells (HPCs) that normally yield erythrocytes, platelets, neutrophils, eosinophils, basophils, monocytes, T and B lymphocytes, natural killer cells, and dendritic cells. While there are examples of distinctive AML with low mutational burden in young patients, such as trisomy 21 (40), multistep leukemogenesis is most apparent from patients with germline mutations as these cases occasionally develop AML later in life after a long latency period (41).

Next generation sequencing (NGS) experiments have revealed that multipotent HSCs harbor clones with recurrent founder mutations in genes involved in global

chromatin changes (e.g. *DNMT3A*, *CEBPA*, *TET2, ASXL1, IDH1/2, IKZF1, SMC1A, CBFB-MYH11*). Moreover, fusion genes are known to arise in the early stages of tumorigenesis (42). While HSCs of AML patients sometimes carry founder mutations such as fusion genes, they predominantly lack proliferative driver aberrations such as *NPM1*, *FLT3*-ITD, *FLT3*-TKD, *KRAS/NRAS,* or *WT1* that are predominantly found from the more committed HPCs (43-46). Accordingly, the initial founder alterations causing preleukemic state have been shown to occur in HSCs and are generally retained at relapse, while the leukemia initiating, driver mutations more frequently arise in committed HPCs such as in granulocyte/macrophage progenitors, common myeloid progenitors or lymphoid primed multipotent progenitors and are frequently lost at relapse (47-50). Based on recent evidence, a subgroup of human AMLs may also arise from T-lymphoid progenitors with multi-lineage potential (51).

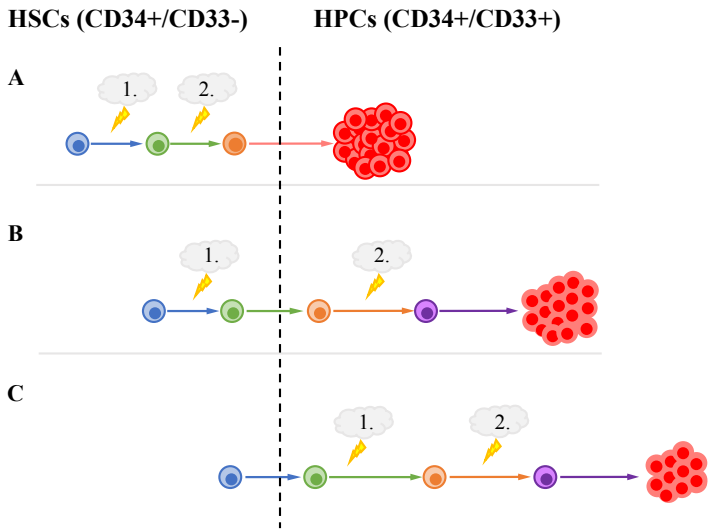

Figure 2 Suggested schemes of leukemogenesis. The drawing illustrates three alternative schemes of how AML arises (A-C). Founder mutations (1.) may strike either HSCs (blue) or myeloid progenitors (green) leading to preleukemic stage. Secondary driver mutations (2.) predominantly strike more committed HPCs (orange) and give rise to LSCs, which turn into leukemic blasts (red). *Adapted from Walter et al, Blood, 2012 (52).*

Shlush *et al* identified preleukemic HSCs with founder mutations from patients in remission indicating that these cells have no response to chemotherapy (43). Similar to preleukemic HSCs, chemoresistance is a known feature of leukemic

stem cells (53). *In vitro* studies have provided evidence showing that AMLs arising from HSCs are significantly more chemoresistant and aggressive than AMLs arising from HPCs (54, 55). Experimental results have also been presented showing that AML patients whose granulocyte/macrophage progenitors carry higher number of HSC-specific mutations have the shortest survival after standard chemotherapy treatment (48). Consistent with the above-mentioned findings, immunophenotyping data from over 200 AML patients showed that high (>1%) CD34+/CD38- blast count, representative of HSC population, correlates strongly with lower post-induction CR rate and shorter disease-free survival (56). Taken together, the above-mentioned findings suggest that therapy and future drug development efforts should be steered toward targeting recurrent founder mutations in preleukemic HSCs or leukemic stem cells (LSCs) rather than proliferative driver mutations.

In most patients, disease etiology cannot be traced back to a specific exposure or inherited genomic alterations. Researchers have postulated that due to the high age of patients at disease-onset, many AML causing mutations may be random events that accumulate during lifetime as a result of endogenous processes. In a landmark work published in 2012, Welch *et al* found that mutations in HPCs accumulate as a function of age (47). More au courant study has pinpointed that clonal hematopoiesis, driven by mutations, increases from 0.8% in individuals below 60 years of age to 19.5% in those who are 90 years of age and above (57). These findings are supported by other reports showing that newly diagnosed AML patients have, on average, three mutations (range 0-9) and that older AML patients usually carry at least one more mutation than younger patients (5, 58).

2.1.2 Diagnosis and classification

During 2011-2015, 967 individuals (475 men and 492 women) were diagnosed with AML in Finland. Of those patients, 65.3% (632/967) were above 65 years of age highlighting that AML is a disease of old age (59). Similar observations have been made in other countries. In the National Cancer Institute (NCI) surveillance, epidemiology and end result (SEER) program of the United States, 57.4% of AML patients (SEER 18, 2011-2015) were 65 years or more with a median age of 68 at diagnosis (60). In United Kingdom, 3126 AML cases were diagnosed in 2015 with 66.5% of them being above 65 years of age (61). The American Cancer Society

estimated that 19,520 new AML patients will be diagnosed in the United States in 2018 (62), but the exact count has not been released yet.

To meet diagnostic criteria for AML, 20% or more blasts (myeloblasts, monoblasts, promonocytes, or megakaryoblasts) should be detected from smears of 500 BM nuclear cells or ≥ 200 blood leucocytes after May-Grünwald-Giemsa or a Wright-Giemsa staining (63, 64). Lower blast counts are sufficient for AML diagnosis if patient carries leukemia-associated mutations (*NPM1, CEBPA, RUNX1, FLT3, TP53,* or *ASXL1*) or cytogenetic abnormalities such as t(15;17), t(8;21), inv(16), or t(16;16) listed on the 2016 WHO classification of myeloid neoplasms and acute leukemia (65).

Many recurrent cytogenetic lesions are detected by mandatory cytogenetic analysis, which should be done with at least 20 BM metaphases. In case of negative result, fluorescent in situ hybridization (FISH) is frequently used for identifying high-risk patients. Quantitative reverse transcription polymerase chain reaction (qRT-PCR) and NGS are routinely used with dedicated gene panels to screen for cryptic translocations and mutations (66). The molecular tests are highly relevant, not only for disease classification and prognostication, but also for generating a treatment plan and taking measures for disease prevention. In addition to molecular genetic tests, immunophenotypic analyses (flow cytometry) and light microscopy are routinely utilized for determining affected cell lineage with various cell-surface and cytoplasmic markers as shown on Table 1 (65, 67). Exome and RNA sequencing has not been adapted to routine diagnostics due to many prevailing challenges related to discrimination of leukemia-related mutations from passenger mutations, germline alterations or PCR-related artefacts, limited sensitivity regarding MRD, and cost (68).

Table 1. *Immunophenotypic markers and cytochemistry used for the diagnosis of AML (Döhner et al modified).*

	Lineage	**Markers**
AML	Precursors	CD34, CD117, CD33, CD13, HLA-DR
	Granulocytic	CD65, cytoplasmic myeloperoxidase
	Monocytic	CD14, CD36, CD64
	Megakaryocytic	CD41 (glycoprotein IIb/IIIa), CD61 (glycoprotein IIIa),
	Erythroid	CD235a (glycophorin A), CD36

Newly diagnosed AML patients are classified based on cellular morphology and genetic abnormalities using two different classification schemes. The French-American-British (FAB) classification (Table 2), introduced in 1976, divides AML patients into eight different disease entities (M0-M7) according to cell morphology and cellular response to histochemical stains (69-71). FAB system is progressively being replaced by the WHO classification scheme (Table 2), which was established in 2001 (72). The FAB system, however, remains a useful complementary assay for patient classification. Contrary to FAB classification, WHO classification is based on causality rather than effect (morphology) and therefore is likely to be more accurate and clinically relevant system. WHO recognizes six classes including (i) AML with recurrent genetic abnormalities, (ii) AML with myelodysplasia-related changes, (iii) therapy-related myeloid neoplasms, (iv) AML not otherwise specified, (v) myeloid sarcoma, and (vi) myeloid proliferations of Down syndrome (73, 74). It is likely that in the near future all AML patients will be classified based on genetic abnormalities, although a fraction of AML patients currently exist with no known driver mutations (5).

Table 2. *WHO and FAB classification of AML and related malignancies.*

WHO Classification	**Features**
1. AML w/ recurrent genetic abnormalities	t(8;21)(q22;q22.1); *RUNX1-RUNX1T1*, inv(16)(p13.1;q22) or t(16;16)(p13.1;q22); *CBFB-MYH11*, APL with *PML-RARA,* t(9;11)(p21.3;q23.3); *MLL3-KMT2A,* t(6;9)(p23;q34.1); *DEK-NUP214*, inv(3)(q21.3;q26.2) or t(3;3)(q21.3;q26.2); *GATA2/MECOM* Megakaryoblastic AML w/ t(1;22)(p13.3;q13.3); *RBM15-MKL1, BCR-ABL1* (provisional), *NPM1, CEBPA* (biallelic), *RUNX1* (provisional)
2. AML w/ myelodysplasia-related changes	Dysplastic features in ≥ 50% of cells in two or more lineages
3. Therapy-related myeloid neoplasms	Earlier treatment with etoposide or alkylating agents
4. AML, not otherwise specified	AML with minimal differentiation, AML with or without maturation, Acute myelomonocytic leukemia, Acute monoblastic/monocytic leukemia, Pure erythroid leukemia, Acute megakaryoblastic leukemia, Acute basophilic leukemia, Acute panmyelosis with myelofibrosis
5. Myeloid sarcoma	Appearance of solid tumour made of myeloid blasts
6. Myeloid proliferations of Down syndrome	Transient abnormal myelopoiesis, Myeloid leukemia associated with Down syndrome
FAB classification	**Morphology**
M0.	Acute myeloid leukemia without differentiation
M1.	Acute myeloid leukemia with minimal differentiation
M2.	Acute myeloid leukemia with differentiation
M3.	Acute promyelocytic leukemia (hypergranular or typical)
M4.	Acute myelomonocytic leukemia
M4v.	Acute myelomonocytic leukemia with BM eosinophilia
M5.	Acute monocytic leukemia
M6.	Acute erythroid leukemia (Erythroleukemia)
M7.	Acute Megakaryoblastic leukemia

2.1.3 Prognostic factors and treatment

Prediction of patient's risk and likelihood of survival has been an important part of medicine since the Book of Prognostics, written around 400 BC by Hippocrates. It is therefore of no surprise that the word prognosis derives from Greek words *pro-*, "before" and *gnôsis*, "inquiry, investigation, knowing". The foreknowledge of how different demographic, clinical and genetic factors identified at diagnosis affect outcome parameters is highly informative and impact treatment decisions. In AML, prognostic factors are roughly divided into patient-related and disease-related factors with latter having the highest prognostic power. The patient-related factors include age, performance status, general health, and comorbidities, whereas disease-related prognostic factors consist of cytogenetic and molecular abnormalities (75). Currently only few factors influence treatment decisions and those that do, mainly tell clinicians whether patient is fit for intensive chemotherapy. Based on the most recent recommendations from the ELN expert panel, all patient-related factors beside age should be considered when deciding whether patient is fit to receive standard chemo-therapy regimen (63, 76).

Fairly recent progress in the management of AML is the establishment of genetic risk groups, which provide solid background for risk stratification (77). The established risk groups (favorable, intermediate, and adverse) formulated by the National Comprehensive Cancer Network (NCCN) and ELN are based on 5-year OS rates, which in the three patient subsets are 55-65%, 24-41%, and 5-14%, respectively (78, 79). Both schemes are highly similar although some differences exist in the intermediate and adverse risk groups. Based on the NCCN version, patients with normal karyotype, trisomy 8, and those carrying c-KIT mutation with t(8;21), inv(16), or t(16;16) should be classified as intermediate-risk in addition to the factors listed on Table 3.

Papaemmanuil *et al* recommended in 2016 that *TP53*, *SRSF2*, *ASXL1*, *DNMT3A*, and *IDH2* should also be incorporated into the risk stratification groups since they are frequent mutated in AML and strong influencers of clinical outcome (5). Two of these mutations, namely *TP53* and *ASXL1*, were recently added to the 2017 ELN risk strafication scheme, however, the ELN panel thought there was insufficient evidence to warrant assignment of other mutated genes such as *DNMT3A*, *IDH1*, or *IDH2* into the risk groups. On-going mutation profiling will continue to refine risk stratification and to facilitate identification of optimal

treatments for each patient. In the future, we may see the addition of *IDH* mutations in the risk groups as they are observed in roughly 20% of AML cases and strongly influence treatment decisions (4, 5). FDA has recently approved two IDH inhibitors (IDH2 inhibitor enasidenib and IDH1 inhibitor ivosidenib) for relapsed/refractory AML patients with *IDH1* or *IDH2* mutation (80, 81).

Table 3. *Prognostic risk stratification of AML (adapted from the ELN and the NCCN).*

Risk group	**2017 ELN Criteria**	**NCCN Guidelines Version 1.2018**
Favorable	t(8;21)(q22;q22.1); *RUNX1-RUNX1T1*, inv(16)(p13.1;q22) or t(16;16)(p13.1;q22); *CBFB-MYH11*, Mutated *NPM1* without *FLT3*-ITD Mutated *NPM1* with *FLT3*-ITD^{low} Isolated biallelic mutated *CEBPA*	Core binding factor: inv(16) or t(16;16) or t(8;21), t(15;17), Mutated *NPM1* without *FLT3*-ITD Mutated *NPM1* with *FLT3*-ITD^{low} Isolated biallelic mutated *CEBPA*
Intermediate	Mutated *NPM1* and *FLT3*-ITD^{high} Wild-type *NPM1* without *FLT3*-ITD or with *FLT3*-ITD^{low} t(9;11)(p21.3;q23.3); *MLL3-KMT2A,* Cytogenetic aberrations not classified as favorable or adverse	Core binding factor with KIT mutation Mutated *NPM1* and *FLT3*-ITD^{high} Wild-type *NPM1* without *FLT3*-ITD or with *FLT3*-ITD^{low} (without poor risk genetic lesions) t(9;11)(p21.3;q23.3); *MLL3-KMT2A*
Adverse	t(6;9)(p23;q34.1); *DEK-NUP214*, t(v;11q23.3); *KMT2A* rearranged t(9;22)(q34.1;q11.2); *BCR-ABL1* inv(3)(q21.3q26.2) or t(3;3)(q21.3;q26.2); *GATA2, MECOM* -5 or del(5q); -7; -17/abn(17p) Complex karyotype, monosomal karyotype Wild-type *NPM1* and *FLT3*-ITD^{high} Mutated *RUNX1,* Mutated *ASXL1,* Mutated *TP53*	Complex karyotype, monosomal karyotype -5, 5q-, -7, 7q-, 11q23- non t(9;11), Inv (3), t(3;3), t(6;9), t(9;22), Normal cytogenetics: Mutated FLT3-ITD, Mutated TP53, Mutated RUNX1, Mutated ASXL1, Wild-type NPM1 and FLT3-ITD^{high}

Majority of fit patients receive standard induction treatment with cytosine arabinoside and an anthracycline (daunorubicin, idarubicin, mitoxantrone, or etoposide) at conventional or high dose. The standard upfront treatment termed 7+3 (7 days of cytarabine at 100-200 mg/m^2 and 3 days of daunorubicin at 60-90 mg/m^2, idarubicin at 12 mg/m^2, or mitoxantrone 7 mg/m^2) is administered 3-4 times with a 4-6 week recovery between treatment blocks. Patients with adverse risk respond poorly to 7+3. The CR rates in fit patients under 60 years and in those 60 or more, receiving 7+3 are 60-80% and 40-60%, respectively (82). Patients

with APL (10-15% of all AML cases) may be cured with all-trans-retinoic acid in combination with arsenic trioxide or chemotherapy, although some controversy exists regarding optimal dose and treatment schedule (83). Newly diagnosed t-AML or AML patients with myelodysplasia-related changes (MRC) are eligible for CPX-351 (liposomal encapsulation of cytarabine and daunorubicin), which received FDA approval in 2017 and EMA approval in 2018. CPX-351 has resulted in longer OS compared to standard 7+3 treatment in patients with t-AML or AML-MRC in randomized clinical studies (84).

Few exceptions to the 7+3 regimen exist: approximately 30% of AML patients carrying *FLT3*-mutation are now eligible for treatment with 7+3 in combination with FLT3/multikinase inhibitor midostaurin (approved by FDA and EMA in 2017) or gilteritinib (approved by the FDA in November 2018) (85). In younger newly diagnosed FLT3-positive AML patients, this induction therapy has led to significantly longer median survival compared to 7+3 alone (74.7 months versus 25.6 months). The large trial that led to midostaurin approval lasted almost 10 years and enrolled over 3000 patients (86). Another exception to 7+3 is that CD33-positive AML patients are eligible for treatment with gemtuzumab ozogamicin (GO), an FDA- and EMA-approved antibody-drug conjugate targeted against CD33, in combination with cytarabine and daunorubicin. GO has been used in the treatment of core binding factor leukemia since the end of 2017 (87). Prevailing challenge with GO and similar compound (vadastuximab talirine) in clinical development is their association with veno-occlusive disease of the liver due to expression of CD33 by the hepatocytes (88).

For intermediate and high-risk AML patients who fail to achieve CR after 7+3 based induction therapy, allogeneic hematopoietic cell transplant (allo-HCT) is a potentially curative treatment option (89). Allo-HCT is also offered for selected patients with intermediate and adverse risk at first CR, but usually not for patients with favorable prognosis (90). Due to serious risks and side-effects, allo-HCT is generally not considered for older unfit AML patients as they have increased risk for treatment related mortality (91).

Older unfit AML patients remain highly challenging to manage and presently lack standardized treatment options (92). The general consensus is that they should receive supportive care with or without low-dose chemotherapy or hypomethylating agents (78). Recent advancement is that they are now eligible

for venetoclax (BCL-2 inhibitor) or glasdegib (SMO inhibitor) treatment in combination with low-dose cytarabine, azacitidine, or decitabine. Both glasdegib and venetoclax were granted FDA approval in November 2018 (80, 93). CR rates (CR/CRi) in elderly treatment-naïve AML patients treated with venetoclax in combination with low-dose cytarabine or hypomethylating agent (decitabine, azacitidine) have been 54 – 73% (94, 95). Beyond targeted therapies described above, other actionable mutations in AML include *KIT* and *BCR-ABL1*. The selection of molecularly targeted therapies at diagnosis against these and other mutations requires faster screening methods as turnaround time for majority of commercial mutational profiles is currently too long (1- to 2-weeks).

2.1.4 Targeted therapies under development

The call for targeted therapies remains unanswered, considering that still roughly 50% of AML patients below 60 years of age and up to 90% of those above 60 will relapse after achieving CR (96, 97). To meet the prevailing challenges, clinical trial pipelines have been loaded with novel biological therapies that have the potential to improve therapeutic success. As an example, two next-generation FLT3 inhibitors, namely crenolanib and quizartinib are currently in active phase III clinical trials. The ongoing phase III trials (NCT02668653 and NCT03258931) will show whether crenolanib or quizartinib are more efficient at inducing CR and lead to longer OS in combination with chemotherapy (in patients with *FLT3*-ITD or *FLT3*-TKD) compared to recently approved midostaurin or gilteritinib (98). In phase II trial of 29 newly diagnosed *FLT3* mutated patients, crenolanib in combination with 7+3 and consolidation led to a highly promising CR rate of 72% after the first induction (99). Efficacy of FLT3 inhibitors in *FLT3* mutated patients appears to be closely linked to mutational burden (100). It has been postulated that first-generation FLT3 inhibitors may be more beneficial at induction when mutational burden is low, while the more specific second generation FLT3 inhibitors may have better clinical efficacy at relapse/refractory stage when the *FLT3*-ITD mutational burden is higher (101).

Additional kinase inhibitors in phase III trials (active or recruiting) include SRC family kinase inhibitor dasatinib and PLK1 inhibitor volasertib, which are both evaluated with and without chemotherapy for AML. In the upcoming years, we may see the approval of additional IDH1 (BAY1436032) or IDH1/2 inhibitors

(AG-881) (102), epigenetic compounds such as HDAC inhibitor pracinostat, second-generation DNMT inhibitor guadecitabine, MDM2 antagonist idasanutlin, or targeted immunotherapies for patients with AML (103). In phase II trial of 50 unfit older AML patients (NCT01912274), combination of pracinostat and azacitidine led to OS rates of 62% and 45% at one- and 2-year time-points, respectively. These percentages are notably better compared to single-agent azacitidine treatment in a similar patient cohort. At present, immune checkpoint inhibitors (nivolumab, pembrolizumab, durvalumab, atezolizumab, and ipilimumab), anti-CD123, anti-CLEC12A antibodies, bispecific T-cell engagers (blinatumomab), and chimeric antigen receptor T-cells against CD33 and CD123/CLL1 are also being assessed in clinical trials. Based on results from ongoing and past trials, it seems likely that more biologically targeted agents will enter clinics in combination with chemotherapy. Moreover, recent research has produced a vista, in which targeting leukemic stem cells in the up-front induction setting seems highly efficient treatment strategy (104).

2.1.5 Towards personalized therapy of AML

Groundwork for personalized therapy of AML has been laid by improved awareness of genetic alterations and molecular heterogeneity. The first personalized therapy for AML was all-*trans* retinoic acid, which in combination with arsenic trioxide leads to permanent cures for most patients with retinoic acid receptor rearrangement (*PML-RARA*) (8). Since then, only few additional personalized therapies have been developed for AML including FLT3 and IDH1/2 inhibitors against *FLT3* and *IDH* mutations, respectively. Recently, BEAT AML initiative, which is the largest published work regarding the topic, discovered several associations between specific inhibitors and mutations (105). Specific findings were that *ASXL1* mutated AML patients have high *ex vivo* sensitivity to HDAC inhibitor panobinostat, NRAS mutated patients to MAPK inhibitors, and *FLT3/NPM1* mutated patients to BTK inhibitor ibrutinib. Moreover, *BCOR/RUNX1* mutated patients had significant *ex vivo* sensitivity to JAK inhibitors and *TP53* mutated patients to oxidative stress inducer elesclomol. Some of these associations and novel targeted agents will be tested in the upcoming and on-going clinical trials such as the BEAT AML® Master Trial.

2.2 *NUP98* rearrangements in AML

Nucleoporin 98 (*NUP98*) gene encodes for a 98-kDa protein, which together with 34 other membrane-bound proteins selectively passes macromolecules (proteins, RNA and ribosome subunits) through the nuclear pore complex (106). The first rearrangement involving *NUP98* was discovered in 1996, when two groups simultaneously discovered t(7;11)(p15;p15.5)/*NUP98-HOXA9* fusion gene in AML (107, 108). Subsequential work has identified at least 32 distinct *NUP98* rearrangements making it a second largest fusion gene network in AML (10). The number of detected *NUP98* rearrangements has consistently increased throughout the past two decades. Apart from AML, *NUP98* rearrangements have been detected from patients with MDS, CML in blast crisis, chronic myelomonocytic leukemia, juvenile myelomonocytic leukemia, acute lymphoblastic leukemia (ALL), bilineage/biphenotypic leukemia, and renal angiomyolipomas (109-113).

The associated partner genes can roughly be divided to those with and without homeobox domains. Majority of the non-homeobox genes contain coiled-coils and few of them, namely *AF10*, *PHF, JARID1A, NSD1, NSD3,* and *MLL*, harbor plant homology domain fingers involved in chromatin recognition. In all *NUP98* rearrangements, N-terminal FG repeat containing portion of *NUP98* is joined to C-terminal part of partner gene with fusion junctions usually located in introns between exons 11-12, 12-13, or 13-14 (109). The reciprocal *NUP98* translocation products are intermittently found from AML patients with 5'-*NUP98* fusion (114-116). With the increasing number of known *NUP98* rearrangements, it is transpiring that diverse hematological neoplasms may be associated with different *NUP98* rearrangements. Therefore, it seems that partner gene may have an important role in determining which disease a patient develops (109). As an example, *NUP98-SETBP1* and *NUP98-IQCG* fusion genes have only been detected from patients with T-ALL. Interestingly, while MDS is known to progress into AML, all of the NUP98 rearrangements detected in MDS have also been found from patients with AML (109). It currently remains unclear whether specific cell types are more prone to particular *NUP98* translocation events than others. Another interesting aspect is that roughly 25% of *NUP98* rearrangements are detected from therapy-related AML patients. This observation implies that exposure to conventional cancer therapies may increase the prevalence of particular *NUP98* rearrangements such as *NUP98-TOP1*, *NUP98-DDX10*, *NUP98-PRRX1,* or *NUP98-PRRX2* (117). Recently, *NUP98*-translocation was

found from a woman with bilateral renal angiomyolipomas and from her healthy three-year old daughter (113). This finding suggests that *NUP98*-translocations are early leukemogenic events that may occasionally occur in the germline.

2.2.1 AML with t(5;11)(q35;p15.4); *NUP98-NSD1*

The t(5;11)(q35;p15.4) translocation, which joins *NUP98* and *NSD1* genes together, was initially discovered by Jaju *et al* in 1999 from three pediatric AML patients with chromosome 11-specific subtelomeric FISH probes (118). The probes captured a reciprocal trade of genetic material between 5q and 11p subtelomeric regions corresponding to *NUP98* and *NSD1*. Within *NUP98*, the precise breakpoint was shown to localize in intron between *NUP98* exons 12 and 13 (119). Two later studies confirmed that *NUP98-NSD1* fusion results from insertion of 5'*NUP98* fraction into the *NSD1-3'* locus. Subsequent work has validated that the t(5;11)(q35;p15.4) translocation is a recurrent event in AML (116, 120, 121). These patients are predominantly CN-AML (78%) with high WBC counts, particularly if *FLT3*-ITD positive, and predominantly have FAB-M4/M5 morphology (116). Ostensibly, *NUP98-NSD1* has also been detected from sporadic cases with MDS and acute biphenotypic leukemia (11, 117).

2.2.2 Prevalence of *NUP98-NSD1*

To uncover the clinical relevance of *NUP98-NSD1* in AML, several studies have assessed its prevalence. In United Kingdom, prevalence of *NUP98-NSD1* in pediatric AML (< 19 years) was 7% (4/54) (122), while in Portuguese and Japanese cohorts the reported percentages have been 5% (1/20) (123) and 4.8% (6/124) (124), respectively. In a combined cohort of 293 pediatric AMLs collected from three study groups (the Dutch Childhood Oncology group, the AML-Berliner-Frankfurt-Münster study group, and the Saint-Louis Children's Hospital), *NUP98-NSD1* was identified from 4.4% (13/293) of cases. The latter study also found that in pediatric CN-AML, *NUP98-NSD1* is present in 16.1% (10/62) of the cases (Figure 3) (116). In Children's Oncology Group (COG) trial patients in the United States, *NUP98-NSD1* was found from 5% (32/683) (120). On the contrary, in Austrian and French pediatric AML cohorts, *NUP98-NSD1* frequencies have been 2% (1/59) (125) and 3% (17/574), respectively (126).

In adult AML, *NUP98-NSD1* is a relatively rare event with a reported prevalence of 1.3-3%. In a combined analysis of German AML SHG 0295 and SHG 0199 trial patients (< 60 years), *NUP98-NSD1* was detected from 1.4% (7/504) (121). In another German cohort, *NUP98-NSD1* was found from 2.1% (8/378) of adult CN-AML patients (127). Consistently, the frequency of *NUP98-NSD1* in the collective Dutch-German-French AML cohort was 1.3% (10/788) in adults and 2.3% (8/344) in adult CN-AML (116). Furthermore, in the South West Oncology Group trial cohort in the United States, the prevalence of *NUP98-NSD1* in adult AML was 3% (7/237) (120), while it was 1.5% (3/200) in the TCGA (The Cancer Genome Atlas) cohort of 200 adult *de novo* AML patients (4). In Canada, *NUP98-NSD1* was identified from 1.7% of adult AML patients (7/415) (128).

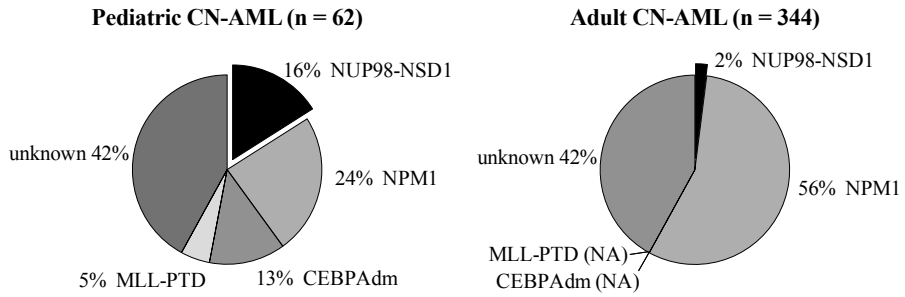

Figure 3 Frequency of *NUP98-NSD1* in pediatric and adult CN-AML. *Adapted from Hollink et al, Blood, 2012 (116).*

2.2.3 Leukemogenesis

As yet, only limited number of studies have investigated how *NUP98-NSD1* fusion may promote leukemic transformation and whether additional mutations are needed for triggering leukemogenesis. Currently, it is known that *NUP98-NSD1*-driven transformation is closely linked to aberrant gene expression and that *NUP98-NSD1* exerts its leukemic functions in the nucleus where it forms nuclear speckles (116, 129, 130). The precise mechanisms of how *NUP98-NSD1* mediates expression changes remain poorly understood. It seems apparent that the N-terminal portion of *NUP98* plays a central role as it is involved in more than 30 unique *NUP98* translocations (109, 111, 112).

In a benchmark work, Wang and colleagues presented that sub-lethally irradiated syngeneic BALB/c mice develop AML after being injected with retrovirally transduced Lin- progenitors expressing *NUP98-NSD1* (129). They discovered that NUP98-NSD1 halts the differentiation of Lin- marrow derived progenitors by enforcing cellular self-renewal and by binding next to *HoxA7* and *HoxA9* genomic loci. They pointed out that at this loci, NUP98-NSD1 activates and maintains the expression of several *Hox-A* genes and *Meis1* by colocalizing CBP/p300 mediated H3/H4 acetylation and H3mK36 of regulatory elements. They concluded that these events disallow EZH2 binding in proximity to *HoxA9* and appearance of H3mK27, which has a critical role in silencing of *HoxA* genes.

The evidence suggesting that NUP98-NSD1 alone induces AML, however, could not be reproduced by Thanasopoulou *et al*. By transplanting *NUP98-NSD1* transduced Lin- marrow progenitor cells (harvested from methylcellulose cultures) into sub-lethally irradiated syngeneic BALB/c mice, they found that *NUP98-NSD1* alone induces a phenotype resembling myeloid hyperplasia (120). On the contrary, they observed that all mice injected with Lin- marrow cells co-expressing *NUP98-NSD1* and *FLT3*-ITD rapidly develop AML. It is therefore likely that *NUP98-NSD1* induces a premalignant phenotype in the HSCs en route to full-blown malignancy upon acquisition of additional cooperative mutations such as *FLT3*-ITD and *WT1* that facilitate complementary effects on cell phenotype.

Recent work has provided additional insights into the leukemogenic mechanisms by reporting that NUP98-NSD1 may be recruited to chromatin adjacent to *HOXA-B* cluster genes and *Meis1* by several mechanisms including interactions with MLL1 (131), Crm1 (132), or Wdr82 and the WSC complex (Wdr82 – Set1A/COMPASS) (133). The above-cited study by Franks *et al* discovered that NUP98-NSD1 promotes aberrant H3K4me3 at its binding sites and thereby drives constitutive up-regulation of various developmental genes linked to AML. Another line of evidence suggests that DOT1L-AF10 complex mediates higher degree of H3K79 methylation and thereby cause constitutive activation of *HOX* cluster genes in *NUP98-NSD1*$^{+}$ cells (134). Additional clues to leukemogenic mechanisms may be provided by coiled-coil regions of NUP98-NSD1 that enable interactions with multiprotein complexes or other transcription factors (135).

2.2.4 Genomic and transcriptomic changes

Roughly 26% (11/42) of *NUP98-NSD1*$^+$ AML patients have comutated *FLT3*-ITD and *WT1*, whereas either *FLT3*-ITD or *WT1* mutation is found from 70- 91% and 29-50% of the cases, respectively (116, 120, 127, 128). Interestingly, *NUP98-NSD1*$^+$*/FLT3*-ITD$^+$ AML patients have also been found with concurrent *MYC* mutations (128) and *NUP98-NSD1*$^+$/*WT1*$^+$ AML patient with concurrent *N-RAS* mutation (116). It seems apparent that *NUP98-NSD1*$^+$ patients rarely harbour less than three genomic alterations. The list of other infrequently detected comutations include *ASXL1*, *CEBPA*, *KIT*, and *K-RAS* (4, 116, 121, 124, 126, 128, 136-138). Although *NUP98-NSD1* is predominantly reported as a sole cytogenetic abnormality, many co-existing cytogenetic aberrations have been reported including del 3q, del 5q, del 9q, del 11p, +6, +8, +13, +21, +22, t(10;19)(q23;q13.4), t(12;15)(p13;q25), an inv (3)(q21q26) karyotype with monosomy 7 (116, 118, 121, 122, 124, 139-141). Further studies are warranted to learn how the various co-mutations or cytogenetic co-alterations may affect therapy responses and patient survival in this biologically distinct subgroup of AML.

Until now, only few studies have explored gene expression changes in *NUP98-NSD1*$^+$ AML patients. Two studies have applied RNA-Seq (128, 142) and three studies microarray analysis with HGU 133 Plus 2.0 array (116, 124) or GeneChip Mouse Genome 430 2.0 array (129). In mouse progenitors transduced with *NUP98-NSD1*, six genes, namely *HoxA5*, *HoxA7*, *HoxA9*, *HoxA10*, *Meis1*, and *Rab38* were shown to be up-regulated 5-fold or more (129). Analyses using *NUP98-NSD1*$^+$ patient samples have confirmed significant overexpression of several *HOX-AB* cluster genes.

According to two microarray analyses, the number of differentially expressed probe sets in *NUP98-NSD1*$^+$ AML patients is lower compared to other AMLs (116, 124). In the microarray analyses, only 15 probe sets were significantly up-regulated in both data sets in addition to *HOX* cluster genes. The most highly up-regulated genes included *NKX2-3*, *VENTX*, *NRG4, FLJ42875, LOC404266, H2AFY2, TRGCA, CPNE8*, *CDCP1*, and *PRDM16*. Recent work by Shiba *et al* has validated *PRDM16* overexpression in a Japanese cohort of *NUP98-NSD1*$^+$ AML patients (n = 11) (143). RNA-Seq based expression analysis by Lavallée *et al* was highly consistent with the two microarray analyses. Interestingly, *NKX2-3, VENTX, FLJ42875, CDCP1, H2AFY2, NRG4, CPNE8,* and *PRDM16* were

shown to be among the 100 most up-regulated genes in *NUP98-NSD1*$^+$ AML compared to non-*NUP98-NSD1* AML cohort. RNA-Seq data from another study showed that expression profile of *NUP98-NSD1*$^+$ patient samples is retained in the xenografts (142). Pathological relevance of the identified comutations and associated transcriptome changes remain largely unstudied.

2.2.5 Prognosis

Already two decades ago when the first three *NUP98-NSD1*$^+$ children were identified, it was surmised that this patient subgroup has poor response to induction chemotherapy and short OS ranging from 10 to 18 months (118). Following the initial observations, aggressive clinical course with a high relapse rate has been shown to be a defining feature of *NUP98-NSD1*$^+$ AML patients and has been correlated with increasing *NUP98-NSD1* expression (116, 122). Although analysed patient cohorts have been relatively small, the reported 3-4-year event-free survival (ranging from 0-33.3%) and OS rates strongly suggest that conventional chemotherapeutic regimen rarely leads to permanent cures free of complications in patients with *NUP98-NSD1* (116, 120, 124, 137). According to Fasan *et al*, the median event-free survival in adult patients with *NUP98-NSD1*$^+$ (n = 6) is 1.8 months compared to 11 months in *NUP98-NSD1*$^-$ cohort (n = 251) (127). Another study provided realworld data suggesting that pediatric patients with *NUP98-NSD1* respond better to first-line treatments than adults. The 4-year OS in a pediatric cohort was shown to be 31%, while it was 11% in adults (116). Similar OS percentages in *NUP98-NSD1*$^+$ pediatric cohorts have been reported by at least two other studies (120, 124).

Majority of AML patients with *NUP98-NSD1* and concurrent *FLT3*-ITD never reach CR (144). In a multi-center trial cohort reported by Ostronoff *et al*, only 28% (9/32) of pediatric AML patients (COG trial cohort) and 20% (1/5) of adults (South West Oncology Group *FLT3*-ITD cohort) with concomitant *NUP98-NSD1* and *FLT3*-ITD achieved CR. The lowest CR rate (9%) was seen in *NUP98-NSD1*$^+$ AML patients with concurrent *FLT3*-ITD and *WT1* mutations (1/11) (120). In line with these findings, a recently published paper, which included nearly 1000 patients showed that *FLT3*-ITD yields markedly inferior outcomes in combination with *WT1* mutations and/or *NUP98-NSD1* compared to patients harboring *FLT3*-ITDs alone or in combination with mutated *NPM1* (145).

3 AIMS OF THE STUDY

The overall objective of this study was to provide insights into the biology and treatment of AML patients with high-risk *NUP98-NSD1* and concomitant *FLT3*-ITD. These patients urgently need for more effective and less toxic treatments as majority of them are unresponsive to standard induction chemotherapy.

The specific aims of this study were:

I. To facilitate the molecular monitoring of *NUP98-NSD1* fusion gene in AML by studying alternative splice variants.

II. To discover novel candidate drugs and drug combinations for the treatment of AML patients with *NUP98-NSD1* fusion and concomitant *FLT3*-ITD.

4 MATERIALS AND METHODS

4.1 Patient material

The patient material consisted of BM aspirates and skin biopsies from patients and healthy donors who had signed written informed consent before sampling. Mononuclear cells (MNCs) were isolated from BM aspirates using Ficoll-Paque Premium™ density gradient centrifugation according to manufacturer's protocol (GE Healthcare, Little Chalfont, UK). All samples were collected in accordance with the updated tenets of the Declaration of Helsinki and with written informed consent. Ethical permits for the study were acquired from the Helsinki University Hospital Ethics Committee (permit numbers 239/13/03/00/2010 and 303/13/03/01/2011).

In study I, chimeric *NUP98-NSD1* transcripts and alternative splicing events were studied from three t(5;11) translocation positive AML patients (600, 3600, and 3660) (Table 4). The control group consisted of four males and six females without t(5;11) translocation. The mean age of the patients and controls at the time of sampling was 46 years (range 32–59.2) and 42.6 years (range 20.4 – 72.2), respectively. The control samples (N = 19) included healthy individuals and patients with AML, MDS, ALL, chronic myelomonocytic leukemia, and CML. RNA sequencing data was analyzed from samples collected at diagnosis (N = 2), relapse (N = 10), refractory stage (N = 6), and remission (N = 1).

In study II, DSRT was performed to BM MNCs from four *NUP98-NSD1*$^+$*/FLT3*-ITD$^+$ AML patients (Table 4), nine *NUP98-NSD1* negative AML patients with *FLT3*-ITD, and ten healthy donors. The median age of *NUP98-NSD1*$^+$ patients at the time of sampling was 54.8 (range 39.8–59.2), while the median age of controls (five males and four females) was 59.8 years (range 27.7–77.8). RNA-seq was performed in parallel to three *NUP98-NSD1*$^+$*/FLT3*-ITD$^+$ AML patients, nine *NUP98-NSD1* negative AML patients with *FLT3*-ITD and BM CD34+ cells from four healthy donors. CD34+ cells were enriched from the healthy donor BM MNCs using EasySep® Human CD34+ Selection Kit (StemCell Technologies, Vancouver, Canada). Exome sequencing was carried out to two *NUP98-NSD1*$^+$*/FLT3*-ITD$^+$ AML patients and phosphor-kinase antibody array (R&D systems, Minneapolis, MN, USA) to one *NUP98-NSD1*$^+$*/FLT3*-ITD$^+$ patient.

Table 4. *Clinical and demographic characteristics of the NUP98-NSD1⁺/FLT3-ITD⁺ study patients at the time of sampling.*

Characteristics	600_2	3600_1	3660_3	7499_2
Gender	Male	Female	Male	Female
Age at diagnosis	54	39	58	32
WHO classification	Acute monocytic leukemia	Acute myeloblastic leukemia with maturation	Acute monocytic leukemia	Acute myeloblastic leukemia with maturation
FAB subtype	M5b	M2	M5	M2
BM blast count	75	40	95	70
Karyotype	46 XY, del 3q, t(12;15) t(5;11)(q35;p15.4)	46 XX, t(5;11)(q35;p15.4)	46 XY, del (9)(q21-22) t(5;11)(q35;p15.4)	46, XX, t(5;11)(q35;p15.4)
FLT3-ITD size (bp)	57	213	57	51 (ITD#1) 57 (ITD#2)
FLT3-ITD allelic ratio (heigh fraction)	0.17	0.28	0.40	0.40
BM immunophenotype	CD33+, CD38+, CD4+, CD13+, CD11b+, HLA-DR+, CD65+, CD14+, CD64+, CD15; a proportion of cells CD177+	CD34+, CD33+, CD3-, CD135+, (weak 24%), TdT+ (28%), CD36+, CD38+, CD13+, MPO+, CD11b+, HLA-DR+, CD117+, CD15+, CD65+, CD79-	CD38+, CD34+, CD9-, CD33+, CD13+ weak (16%), CD16-, MPO+, CD11b+ (26%), HLA-DR+, CD19-, cyCD3-, NG2-, CD14-, CD25+, cyCD79a-, CD117+, CD56-, CD2+ (26%), CD203c, CD15+ (21%) CD42a&61-, CD123+, CD105+, IREM2-, CD4+ weak (36%), CD64-, CD71+, CD7-, CD36+, CD133-, TdT+, CD41a, CD42b-,CD22+, CD135+ weak, CD96+ weak (66%)	CD34+ (48%), CD33+, CD117+, HLA-DR+, MPO+, CD19-, CD7+, CD4-, CD3-, CD13-

4.2 Murine cell models

4.2.1 Cloning and Sanger sequencing

Total RNA (1 µg) from index patient's BM MNCs was reverse transcribed to cDNA using SuperScript™ III First-Strand Synthesis System for reverse transcription PCR with Oligo (dT) primers (Thermo Fisher Scientific). *NUP98-NSD1* was amplified from cDNA using primers 297/298 (Table 2) with Phusion™ (HF) DNA polymerase (Thermo Fisher Scientific). PCR protocol was as follows: 95°C for 2 min, 35 cycles of denaturation at 95°C for 20 s, annealing at 54°C for

10 s, and elongation at 72°C for 100 s with a final extension at 72°C for 5 minutes. Amplified fragments were separated on 1% agarose gel electrophoresis with SYBR® Safe DNA stain (Thermo Fisher Scientific) and extracted using NucleoSpin® Gel and PCR Clean-up Kit (Macherey-Nagel, Duren, Germany). Fragments corresponding to *NUP98-NSD1* were ligated into pCR® 2.1-TOPO® vectors using TOPO™ TA Cloning™ Kit and transformed into One Shot™ TOP10 Chemically Competent *E. coli* based on manufacturer's protocol (Thermo Fisher Scientific). After overnight incubation at +37°C, NUP98-NSD1^{+} colonies were identified from LB + ampicillin (100 µg/ml) agar plates with colony-PCR. Positive colonies were cultivated overnight at +37°C. Next day, plasmids were extracted with NucleoSpin® Plasmid Easy Pure Kit (Macherey-Nagel) and Sanger sequenced bidirectionally (with primers described on Table 5) using ABI370xl DNA Analyzer and BigDye Terminator v3.1 Cycle Sequencing Kit (Applied Biosystems, South San Francisco, CA, USA). Nucleotides were called using Sequencing Analysis v5.2 software and trace files analyzed in Sequencher™5.2 (Gene Codes Corporation, Ann Arbor, MI, USA). Nucleotide sequences were aligned against NCBI (National Center for Biotechnology Information) reference sequences (NM 139131.3 and NM 022455.4) to assemble full-length *NUP98-NSD1* sequences.

In study II, *NUP98-NSD1* transcripts were subcloned from pCR® 2.1-TOPO® vectors into pLeGO-iCER2 lentiviral expression vectors. Briefly, *NUP98-NSD1* fusions were amplified with Phusion™ HF DNA polymerase using primers 297/298. PCR products were purified by mixing twith 3 M NaAc (2µl) and 99% EtOH (60 µl). The mixture was centrifuged at 14,000 rpm for 5 minutes and supernatant discarded. The pellets were washed twice with 70% ethanol and dried for 5 minutes at 70°C before exposing them to T4 polynucleotide kinase (10U/µl) following manufacturer's protocol (Thermo Fisher Scientific). The pLeGO-iCER2 vector was digested with Stu I restriction enzyme (10U) (New England Biolabs, Ipswich, MA, USA). T4 PNK treated insert cDNA and Stu I digested plasmid were resolved on 1% agarose gel and extracted using Nucleospin® Gel and PCR Clean-up Kit (Macherey-Nagel, Duren, Germany). The plasmid DNA was treated with FastAP Thermosensitive alkaline phosphatase (Thermo Fisher Scientific). Overnight ligations were performed using T4 DNA Ligase (New England Biolabs). Stbl3 Chemically Competent *E. coli* cells were heat-shock transformed with ligated expression vectors and plated on LB+ampicillin (100 µg/ml) agar plates for overnight incubation at +37°C. Positive clones were

identified with colony-PCR. Plasmid extractions and Sanger sequencing was performed to identify clones with *NUP98-NSD1* transcripts in correct orientation.

Table 5. *Oligonucleotide primers applied for PCR and capillary sequencing.*

Primer	Primer name	Sequence (5'->3')	GC (%)	Tm (°C)
24	M13F	GTAAAACGACGGCCAGT	52.9	58.7
25	M13R	CAGGAAACAGCTATGAC	47.1	50.7
82	AML.600_cDNA_-F	AGCCTTTGGGGCCCCTGGATTTA	56.5	74.2
83	AML.600_cDNA_-R	CCAAAAGCCACTTGCTTGGCTTCC	54.2	73.7
297	NUP98-NSD1-FL-F	ATGTTTAACAAATCATTTGG	25.0	54.0
298	NUP98-NSD1-FL-R	CTACTTCTGTTCTGATTCTG	40.0	51.2
307	seq_NSD1-R2	TTAACATGCTCATGATTTCGG	38.1	62.4
308	seq_NSD1-F2	CTGTGTCCGCTGTCCTGTGG	65.0	69.5
309	seq_NSD1-R3	TTCTTGCAGGAGACGAGC	55.6	62.0
310	seq_NSD1-F3	AGGCCAAAGAATCAACCC	50.0	61.5
311	seq_NSD1-R4	CCTGGGGTCTGCTCAGC	70.6	65.0
312	seq_NSD1-F4	AGCAAAGGTCTGGGGCATAT	50.0	64.5
400	NSD1-seq-B	TCCTTGGTTTCCAGCCAGAG	55.0	66.5
401	NSD1-seq-A	CTGGCCTGGGTGAGTGATTT	55.0	66.3
402	NUP98-NSD1-C	TTGGCACAAATACCAGTGGG	50.0	65.6
403	NUP98-NSD1-D	CGGGATCGTGTTCTACACCT	55.0	63.9

4.2.2 Transduction

Lentiviral packaging of pLeGO-iCER2 (Addgene No. 27346), pLeGO-iCER2-*NUP98-NSD1* expression vectors was done in HEK293T cells. Briefly, an hour before transfection DMEM (Lonza, Basel, Switzerland) complete (10% fetal bovine serum, 1% Penicillin-Streptomycin, 1% L-glutamine) was replaced with 9 ml of Gibco™ OPTI-MEM I™ (Thermo Fisher Scientific). Expression vector pLeGO-iCER2 (10 µg), pCMV, dr8.74 (5.3 µg) (Addgene No. 22036) and pCMV-VSV-G (3 µg) (Addgene No. 8454) were co-transduced into 70-80% confluent HEK293T cells using FuGENE® HD reagent following manufacturer's protocol (Promega, Fitchburg, WI). After overnight incubation at +37°C, OPTI-MEM I™ was replaced with DMEM complete. Viral supernatants were collected twice during 48-hours and filtered with 0,45 µm syringe filter (Sarstedt, Nümbrecht, Germany) into 100,000 MWCO Vivaspin 20 columns (Sartorius, Hamburg, Germany). Viral particles were concentrated (20X) by centrifugation

in KUBOTA 7780 High Speed Refridgerated Centrifuge (KUBOTA, Osaka, Japan) at +4°C for 60 minutes at 3000 rpm. Ba/F3 and 32D cells were transduced with lentiviruses (carrying either empty pLeGO-iCER2 or pLeGO-iCER2-NUP98-NSD1) on 6-well tissue culture treated plates by adding 0.5 ml of fresh or cryopreserved viral concentrate on 200,000 cells in the presence of polybrene (0.8 µg/ml). Transduced cells were expanded in RPMI 1640 complete medium supplemented with mouse IL-3 (10ng/ml). Presence of replication competent virus was excluded 10-14 days later at functional genomics unit.

Retroviral packaging was done in HEK293T Lx cells. Expression vectors were mixed with third generation packaging plasmid in 2:1 molecular ratio. DNA complexes were formed by mixing plasmids with 25 µl TurboFect (Thermo Fisher Scientific) and serum free medium (1 ml). Mixture was incubated at room temperature for 20 minutes and added on HEK293T Lx cells. After overnight incubation at +37°C, medium was changed to DMEM complete. 24 hours later, viral supernatants were collected and filtered into Vivaspin 20 columns (Sartorius). Viruses were concentrated by centrifuging for 45 minutes at 3000 rpm. Viruses were snap-frosen in liquid nitrogen and stored at -80°C until use.

BM cells were isolated from bones of BALB/c mice. Cells were filtered and treated with red blood cell lysis buffer for 10 minutes on ice. Lineage depletion of the BM cells was done using Mouse Cell Lineage depletion kit (R&D systems, Minneapolis, MN, USA). BALB/c Lin- cells were transduced on 6-well plates by adding retrovirus (1 ml) to 2ml medium with cells (500,000 cells/well) in the presence of polybrene (2 µg/ml). The plates were sealed with parafilm and spinned for 90 min at 2500 rpm. After 3-hour recovery in incubator, cells were washed with 1xPBS and placed in RPMI complete medium supplemented with mIL-3 (6 ng/ml), IL-6 (10 ng/ml), and mSCF (10 ng/ml). *NUP98-NSD1*$^{+}$ cell selection was done by incubating the cells with 0.8 mg/ml neomycin (Gibco Geneticin G418 sulfate) for 9-14 days as described (146).

4.2.3 Fluorescence-activated cell sorting

Lentivirally transduced Ba/F3 and 32D cells expressing NUP98-NSD1 or empty plasmid vector were sorted by fluorescence activated cell sorting using BD Aria IIu (BD, Franklin Lakes, NJ, USA) high-speed cell sorter based on cerulean

fluorescence protein (CFP) expression. CFP was excited with 405 nm laser and emission captured with 530/30 bandpass filter. Doublets were excluded based on the forward scatter (FSC-A/FSC-H). CFP positive cells were sorted into 15ml tubes and expanded for further analysis. Green fluorescent protein (GFP) positive BALB/c cells, transduced with pMSCV-IRES-GFP or pMSCV-FLT3-ITD-IRES-EGFP containing retroviruses, were sorted with BD Influx.

4.3 Molecular profiling

4.3.1 Drug sensitivity and resistance testing

Drug sensitivity and resistance testing (DSRT) measures how sensitive or resistant different cells are to various compounds. In this thesis, cell viability-based high-throughput DSRT assay was performed to primary patient cells and experimental cell lines using up to 306 anti-cancer drugs targeting wide range of molecular targets. Drugs were acquired from commercial sources as described in study II and consisted of FDA, PMDA, and EMA approved drugs (45%), investigational compounds (33%), and probes (22%). Briefly, drugs were reformatted on tissue culture treated 384-well flat clear bottom white polystyrene microplates (Corning, New York, NY, USA) in five to eight concentrations over a 10,000-fold concentration range (e.g. 0,1-1,000 nM) using an Echo 550 acoustic dispenser (Labcyte Inc, Sunnyvale, CA, USA). The water-soluble compounds were diluted in water and other compounds in dipolar aprotic solvent (100% dimethyl sulfoxide). To ensure compound activity, drug plates were held in pressurized StoragePods® (Roylan Developments Ltd., Fetcham, UK) under inert nitrogen gas until use or a maximum of four weeks from plate preparation.

Cells were counted using Countess™ automated cell counter (Thermo Fisher Scientific) and dispensed on assay plates at a concentration of 1,500 to 10,000 cells in 20 µl. Prior to adding cells, drugs were solubilized in 5 µl of culture medium. Assay plates were centrifuged after each liquid handling step to place liquids on the bottom of each well and agitated with Titramax 1000 platform shaker (Heidolph, Schwabach, Germany) at 450 rpm for 5 min. For pilot combinatorial screens, dasatinib was added on the wells within 5 µl of priming solution at 500 nM (final concentration 100 nM/25 µl). All liquid handling steps

were done with a peristaltic Multidrop™ Combi Reagent Dispenser (Thermo Fisher Scientific). After each assay set-up, drug plates were incubated in a humidified incubator at +37°C for 72 hours. Cell viabilities were measured with CellTiter-Glo® reagent (25 µl/well) according to manufacturer's protocol (Promega, Madison, WI, USA). Luminescence from each well was quantified with PHERAstar® FS microplate reader (BMG Labtech, Offenburg, Germany). Luminescence data was normalized to positive (100 µmol/L benzethonium chloride) and negative (100% dimethyl sulfoxide) control wells to generate dose-response curves for each drug based on normalized cell survival. The data quality was assessed with a Z-prime statistic (147). Curves were fitted in Dotmatics Browser v4.8 (Dotmatics Ltd., Herts, UK) or in Breeze (in-house platform) using a four parametric logistic fit function that considers slope of the curve, top and bottom asymptote, and inflection point. Outliers were excluded manually. Subsequently, drug sensitivity score (DSS) was calculated for each drug from area under the curve beween 10% and 100% inhibition (relative to the total area) by applying previously described mathematical algorithms (148, 149). Patient-specificity of the drugs was assessed using a selective DSS (sDSS), which indicates the difference in DSS between median of healthy controls and DSS of each patient sample. Likewise, drug specificities in cell lines were evaluated by subtracting DSS of mock-transduced cells from transduced cell lines. Synergy scores (δ) for various drug combinations were calculated in SynergyFinder using a zero-interaction policy method (150, 151).

Drug responses were initially compared between *NUP98-NSD1*$^{+}$*/FLT3*-ITD^{+} BM MNCs from four AML patients and healthy donor BM MNCs to identify hits. The hits were further evaluated in the context of *NUP98-NSD1*$^{-}$*/FLT3*-ITD^{+} AML patients to discover potential candidate compounds. *In vitro* proof-of-efficacy studies were carried out using experimental cell lines. Selective responses were assessed for each drug class to capture significant differences in sensitivities between cells expressing *NUP98-NSD1* and *FLT3*-ITD alone or in combination.

4.3.2 RNA sequencing

Total RNA was extracted from BM MNCs and BM CD34+ cells using RNeasy Mini Kit (Qiagen, Hilden, Germany) or Total RNA Purification Kit (Norgen Biotek, Thorold, Canada). RNA integrity numbers were assessed using 2100

Bioanalyzer with RNA Nano or Pico chips (Agilent Technologies, Santa Clara, CA, USA). Ribo-Zero rRNA Removal Kit (Epicentre, Madison, WI, USA) was used for removing ribosomal RNAs from RNA samples. Next, RNA was purified with RNeasy® MinElute® Cleanup Kit (Qiagen) and reverse transcribed into double stranded cDNA with Superscript® Double-Stranded cDNA Synthesis Kit (Thermo Fisher Scientific) with random hexamers (New England Biolabs). Sequencing libraries were bar-coded with Nextera (Epicentre) or ScriptSeq technologies (Illumina, San Diego, CA, USA) and enriched with ligation PCR according to manufacturer's protocol (Illumina). After size selection (350-700 bp) from agarose gel (2%), fragments were column purified with QIAquick gel extraction kit (Qiagen) and sequenced with Illumina HiSeq™2000 or HiSeq™2500.

In study I, the average length of paired FASTQ reads was 317 nucleotides per mate (range, 104-530 bp). Reads were initially aligned against human reference (GRCh38) using TopHat v2.0.3 and extracted using Perl scripts (152). Extracted reads were executed in FusionCatcher and inspected in integrative genomics viewer to detect *NUP98-NSD1* supporting reads (153, 154). To overcome detection, quantification, and visualization limits, an artificial FASTA format *NUP98-NSD1* reference sequence was created. Therefore, *NUP98* (NM 139131.3) and *NSD1* (NM 022455.4) sequences were extracted from PubMed (NCBI database) and annotated using a general feature format annotation file, which was necessary to create for aligning FASTQ reads with artificial fusion correctly. Aligned reads were extracted and processed by removing PCR duplicates, non-primary reads, and reads with low mapping quality (< 10). Final read counts were acquired using SAMtools (155).

In study II, FASTQ reads were aligned against human (GRCh38) or mouse (BALB/c) reference genome using STAR aligner (gap-aware) together with EnsEMBL reference gene models (Ensembl v82) (156). The normalization of unprocessed FASTQ reads was done using trimmed mean of M values method. The log2 CPM values were calculated using EdgeR R package (3.18.1.) (157). The normalized log2 CPM values of specific drug target genes were compared between *NUP98-NSD1*$^{+}$*/FLT3*-ITD^{+} AML patients, healthy donor BM CD34+ cells, and *NUP98-NSD1*$^{-}$*/FLT3*-ITD^{+} AML patients. Similar comparisons were made with experimental BALB/c cells. Unsupervised hierarchical clustering of mean centered *HOX AB*-cluster gene expression (log2 CPM) in different samples

was done based on euclidean distance using complete linkage method. The heatmaps were generated using R package pheatmap (1.0.8.).

4.3.3 Array Comparative Genomic Hybridization

For array comparative genomic hybridization (A-CGH), three micrograms of genomic DNA from index AML patient was digested and labelled as previously described (158). Genomic DNA was extracted from the BM MNCs with DNeasy Blood & Tissue Kit or QIAamp DNA Mini Kit (Qiagen). The processed DNA was hybridized to Human CGH (244K) Microarrays (Agilent Technologies) containing up to $1x10^6$ 60-mer oligonucleotide probes according to standard procedure from the manufacturer. Copy number variations were analysed with Genomic Workbench software version 5.0 (Agilent Technologies).

4.3.4 Exome sequencing

Exome sequencing was performed to 1-3 µg of genomic DNA isolated from patient 600 and 3660 using DNeasy Blood and Tissue Kit or AllPrep DNA/RNA/ Protein Mini Kit (Qiagen). Exomes were captured and sequenced with NimbleGen SeqCap EZ v2 capture kit (Roche NimbleGen, Madison, WI, USA) using an Illumina HiSeq™ 2500 instrument. The bioinformatic pipeline for mutation calling, annotation and data analysis has been previously described (149, 159).

4.3.5 Fragment analysis

The *FLT3*-ITD allelic burden and ITD lengths in *NUP98-NSD1*$^+$/*FLT3*-ITD$^+$ AML patients were assed using fragment analysis. Briefly, *FLT3*-ITD region from each patient was amplified using 10ng of genomic DNA with PCR primers: 5'-6FAM GCAATTTAGGTATGAAAGCCAGC-3' and 5'-CTTTCAGCATTTTG ACGGCAACC-3' as previously described (160). PCR products were diluted 1:100 and 1:200 in milliQ-water and 2 µl of each dilution was mixed with 10 µl of reaction mix (1 ml Hi-Di mixed with 2.5 µl size standard). Fragment analysis runs were performed with ABI3730xl DNA analyzer. Data was analyzed by

measuring ratio of amplified peak heights and areas between wildtype *FLT3* and *FLT3*-ITD with GeneMapper v5.

4.3.6 Phospho-flow

Experimental BALB/c BM cells were fixed with 1.5% formaldehyde for 15 minutes at +37°C and permeabilized with 100% methanol (30 minutes at -20°C). The permeabilized cells were washed with 1xPBS and stained using Alexa 647-anti-phospho-Stat5 (pY694) and PE-anti-phospho-Erk1/2 (pT202/pY204) (BD Biosciences) antibodies. The samples were run on IntelliCyt iQUE Screener PLUS instrument (Sartorius, Göttingen, Germany) and data analyzed with FlowJo software version 10 (TreeStar, San Carlos, CA, USA).

4.4 Statistical analysis

All statistical analyses were performed in GraphPad Prism version 6 (GraphPad Software, La Jolla, CA, USA). In study I, alternatively spliced intragenic regions were compared between *NUP98-NSD1*$^{+}$ and negative samples using unpaired nonparametric Mann-Whitney U tests. In study II, correlation analyses were done using Spearman's rank correlation coefficient method, and the DSS comparisons between patients and healthy BM MNCs using Mann-Whitney U test. The gene expression values (log2 CPM) were compared between different samples using unpaired two-sample t tests. In all statistical tests, two-tailed P values below 0.05 were considered significant.

5 RESULTS

5.1 Molecular characterization of NUP98-NSD1 (I)

5.1.2 Discovery of *NUP98-NSD1* transcript variants

Due to submicroscopic size and localization in the subtelomere region, t(5;11)(q35;p15.4) translocation cannot be captured with routine G-banding. The detection of this chromosomal aberration relies on accurate molecular monitoring methods such as FISH, RT-PCR or RNA-Seq. In study I, our aim was to facilitate the molecular detection of *NUP98-NSD1* from AML patients with t(5;11) translocation. We focused on RNA splicing, since prior study had reported two chimeric *NUP98-NSD1* transcripts from a patient with myelodysplastic syndrome (11). The index patient for this study was a 54-year old Finnish male from which RNA-Seq had revealed a chimeric *NUP98-NSD1* fusion gene (149). We initially performed A-CGH analysis and found microdeletions within *NUP98* at 11p15.4 and *NSD1* at 5q35.2 indicative of unbalanced t(5;11)(q35.2;p15.4) translocation. The microdeletions at these sites were 0.11 Mb (chr11: 3,617,261-3,723,126) and 0.05 Mb (chr5: 176,546,244-176,595,458) in size as shown in Figure 4.

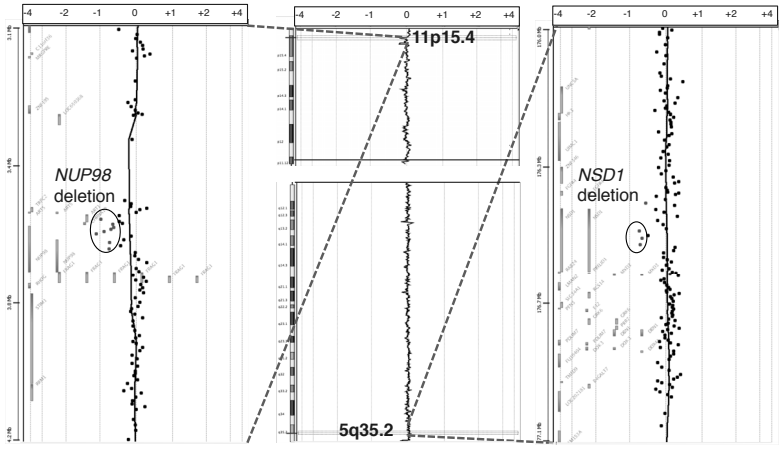

Figure 4 A-CGH graph shows micro-deletions within *NUP98* and *NSD1* genes at 11p15.4 and 5q35.2 from the DNA of index patient compared to reference genome (Hg19). The oligos on the left side of moving average (circles) with copy number ratio below -0.5 indicate sites of heterozygous microdeletions.

Based on the A-CGH analysis, we concluded that putative intronic breakpoints had occurred in DNA within a probe length (60-mer) from positions chr11:3,723,126 (*NUP98*) and chr5:176,595,458 (*NSD1*). We subsequently cloned full-length *NUP98-NSD1* sequences from the index patient's BM MNCs into One Shot™ Stbl3™ chemically competent *E. coli* and Sanger sequenced numerous plasmid clones. Two in-frame and one out-of-frame *NUP98-NSD1* transcripts were found, which were 5,676, 5,562, and 5,432 nucleotides in length. Sequence alignment showed two alternative fusion junctions joining *NUP98* exon 12 to *NSD1* exon 6 and *NUP98* exon 11 to *NSD1* exon 6. We also captured alternative 5' donor site from *NUP98* exon 7 (nucleotides 757-783, amino acids QNKTAFGTS) and skipping of *NSD1* exon 7 (nucleotides 3922-4192) (Figure 5A). The nucleotide numbers were calculated from the first ATG start codon of NCBI reference sequences NM 139131.3 and NM 022455.4.

We searched for additional knowledge about the potential functional consequences of splice events by converting *NUP98-NSD1* sequences into amino acid sequences using EMBOSS Transeq. The two in-frame transcripts harbored same NSD1 functional domains, while the out-of-frame *NUP98-NSD1* transcript lacked all C-terminal domains of NSD1 due to early stop codon. As shown in Figure 5, the number of FG repeats varied between 38, 36, and 39 in the three different NUP98-NSD1 fusion proteins. The tentative amino acid lengths of the three different NUP98-NSD1 fusions were 1891, 1853, and 531, respectively.

5.1.3 Bioinformatic validation of splice events

We re-analyzed RNA-Seq data from index patient since initial alignment had exposed only one NUP98-NSD1 fusion transcript. Strikingly, modified alignment strategy revealed the expression of novel splice events and confirmed that these were not PCR artefacts or RNA-Seq library preparation errors (Figure 6). Of the FASTQ reads spanning across fusion junction, the percentage of reads supporting *NUP98* exon 12 to *NSD1* exon 6 fusion was 93% (75/81) in relapse sample 600_2, while it was 91% (71/78) in the refractory sample 600_3 collected 2 months later. Correspondingly, the percentage of reads supporting *NUP98* exon 11 to *NSD1* exon 6 junction increased from 7% (6/81) to 9% (7/78). Encouraged by these results, we performed RNA-Seq to three additional samples from two adult AML patients with t(5;11). Both fusion junctions were captured from all subsequent

samples confirming that previous studies regarding *NUP98-NSD1*$^{+}$ AML had overlooked the fusion joining *NUP98* exon 11 to *NSD1* exon 6. Similar to index patient, percentage of reads supporting *NUP98* exon 11/*NSD1* exon 6 junction increased from 9.4% (9/96) to 18.1% (13/72) in patient 3660 during disease progression. Concurrently, the relative frequency of the more highly expressed *NUP98* exon 12/*NSD1* exon 6 fusion decreased from 90.6% to 81.9%. In patient 3600, the *NUP98* exon 12 to *NSD1* exon 6 fusion was also the predominant transcript (Figure 4A). Reciprocal *NSD1-NUP98* was not found from any t(5;11)$^{+}$ AML patient indicating 5'-*NUP98-NSD1*-3' as the sole initiating oncogene.

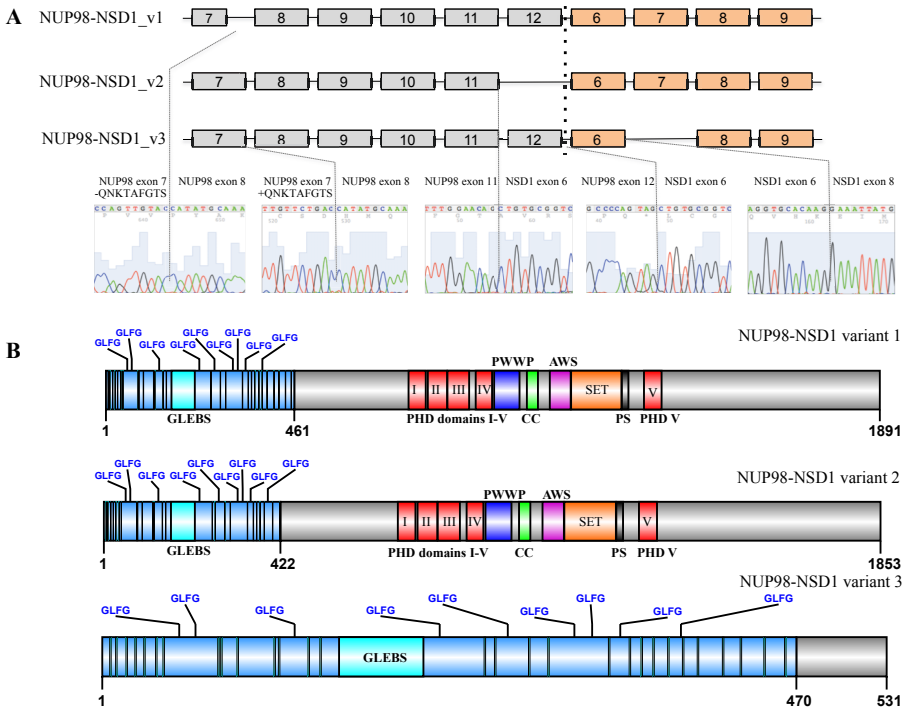

Figure 5 Three alternatively spliced *NUP98-NSD1* transcripts were identified from index patient's leukemic BM cells by cloning and capillary sequencing. (A) The schematic drawing shows spliced intragenic areas (*NUP98* grey, *NSD1* orange) with corresponding nucleotide sequences, whereas the lower panel (B) shows protein structures. The blue color indicates amino acids belonging to NUP98 and grey those that are part of NSD1. The vertical lines (black) represent FG repeats. The distinct protein domains are shown for each protein with amino acid lengths.

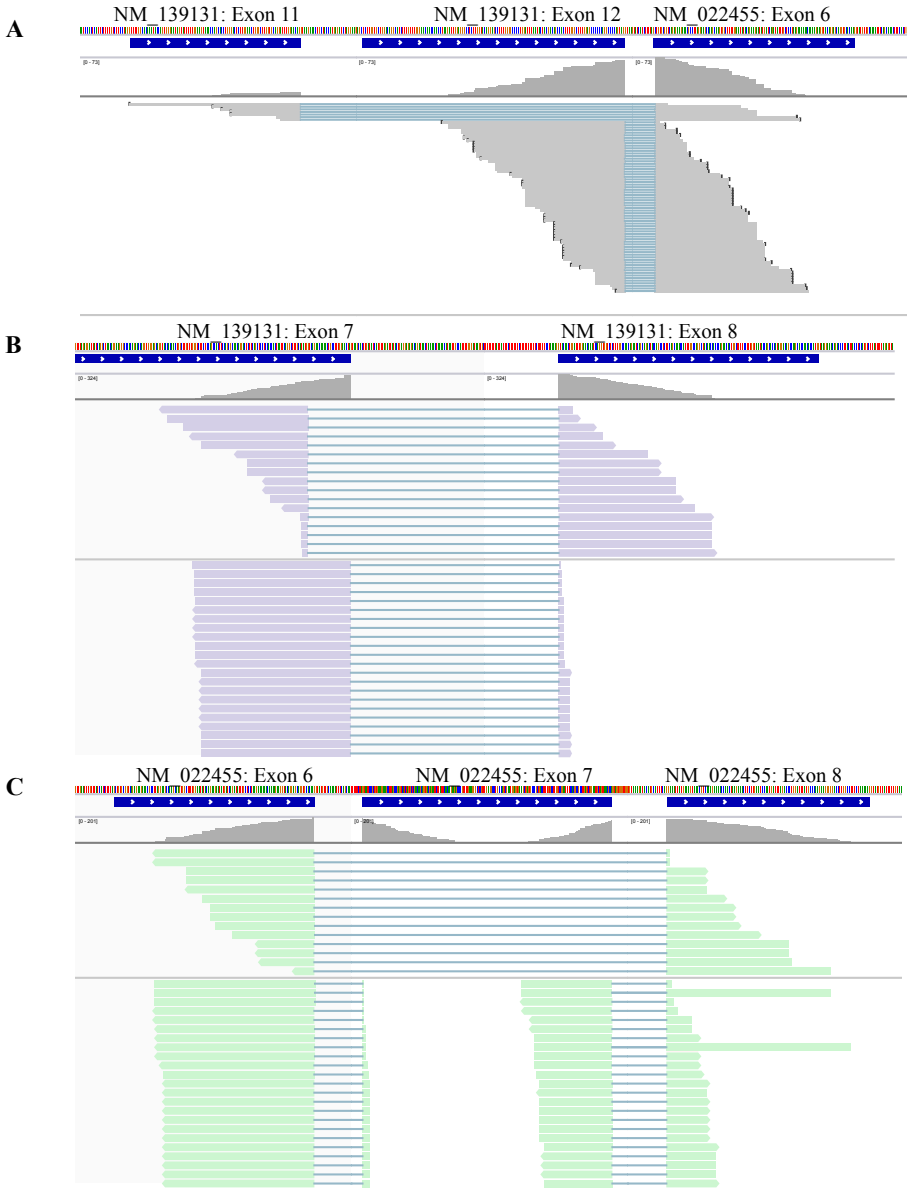

Figure 6 Aligned FASTQ reads. (A) Paired-end reads from the index patient supporting the two alternative fusion junctions, (B) alternative 5' donor site of NUP98 exon 7, and (C) skipping of NSD1 exon 7.

To study whether intragenic splice events are specific to *NUP98-NSD1*-positive disease, we compared the percentage of intragenic splice events between t(5;11) positive (n = 5) and negative samples (n = 16). The t(5;11) negative BM MNCs were collected from patients with different hematological malignancies, and from CD34+ enriched BM cells of two healthy donors. Interestingly, no differences were found in the frequency of alternative 5'donor site of *NUP98* exon 7 or *NSD1* exon 7 skipping between *NUP98-NSD1*$^{+}$ and *NUP98-NSD1* negative patients. The intragenic splice events in *NUP98* and *NSD1* genes were identified from all *NUP98-NSD1* negative cases. The percentage of reads supporting the alternative 5'donor site in the *NUP98-NSD1*$^{+}$ group (n = 5) was 8% (95% CI 5.3-9.9%), while it was 6% (95% CI 5.3-7.4%) in the control group (n = 16). The percentage of reads supporting *NSD1* exon 7 skipping was 6% (95% CIs 0-13.1% and 3.4-9.4%) in both groups. Differences in intragenic splicing of *NUP98* or *NSD1* were insignificant between the positive and negative groups (Figure 7B-C).

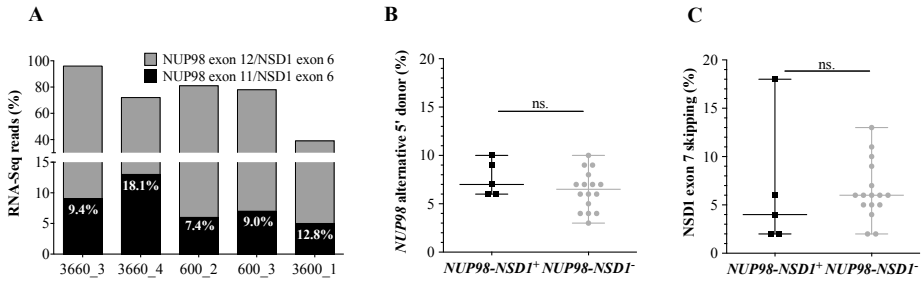

Figure 7 FASTQ read counts supporting the two alternative fusion junctions and intragenic splice events. (A) The graph shows the total number of read supporting the two fusion junctions in three de novo AML patients with the cryptic t(5;11)(q35;p15.4) translocation. (B-C) The scatter plots illustrate the percentage (y-axis) of reads supporting alternative 5'donor site of *NUP98* exon 7 and skipping of *NSD1* exon 7 relative to all reads covering these exonic regions in *NUP98-NSD1*$^{+}$ (N = 5) and *NUP98-NSD1*$^{-}$ (N = 16) patient samples. Error bars show mean with range.

5.2 Novel therapy options for *NUP98-NSD1*$^{+}$ AML (II)

5.2.1 Drug sensitivities in experimental cell lines

In study II, our objective was to discover clinically relevant and more efficient treatment options for *NUP98-NSD1*$^{+}$/*FLT3*-ITD^{+} AML patients. The study was initiated by establishing experimental mouse cell lines (BALB/c and BA/F3) that express NUP98-NSD1, FLT3-ITD, or both together. We first analyzed differential drug sensitivities in the mouse cell lines based on drug mechanism of action. As shown in Figure 8, we discovered that leukemic NUP98-NSD1^{+}/FLT3-ITD^{+} cells have significantly lower sensitivity to BCL-2 inhibitors (P = 0.029) compared to cells expressing NUP98-NSD1 alone, which had particularly high sensitivity to BCL-2 inhibitors. Another striking observation was that dual positive cells have significantly higher sensitivity to FLT3 and MEK inhibitors ($P < 0.01$) compared to cells expressing FLT3-ITD alone. Analysing single therapeutic agents from these drug classes, we found that pan-BCL-2 inhibitor navitoclax had the highest mean sDSS ($\overline{x} = 17.5$) in the NUP98-NSD1^{+} mouse cells, while FLT3 inhibitor quizartinib (mean sDSS = 22.8) and MEK inhibitor pimasertib (mean sDSS = 13.2) had the highest efficacy against *NUP98-NSD1*$^{+}$/*FLT3*-ITD^{+} cells.

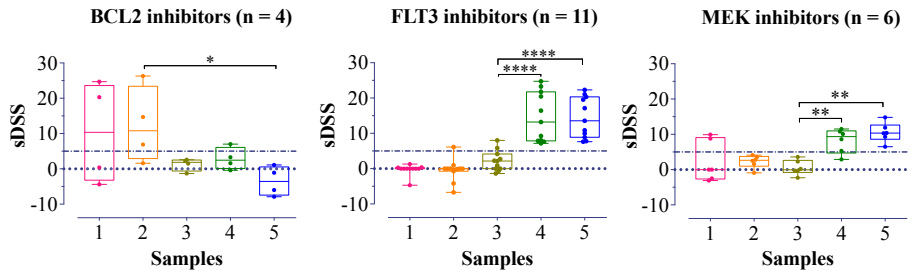

Figure 8 DSRT data showing molecularly specific drug responses in experimental mouse cell lines. The numbers below each graph indicate different cell lines: 1, Ba/F3 NUP98-NSD1; 2, BALB/c NUP98-NSD1; 3, BALB/c FLT3-ITD; 4, BALB/c NUP98-NSD1 + FLT3-ITD (preleukemic); 5, BALB/c NUP98-NSD1 + FLT3-ITD (leukemic).

To follow-up on the FLT3 and MEK inhibitor sensitivities and learn about the biological mechanisms leading to these responses, we performed phospho-flow analysis. We evaluated phosphorylation of STAT5 and ERK1/2, since earlier studies had shown that co-activation of STAT5 and MAPK-pathways occurs

downstream of activated FLT3 signaling (161). Intriguingly, the highest phosphorylation of STAT5 and ERK1/2 was found in the cells co-expressing NUP98-NSD1 and FLT3-ITD coinciding with the highest FLT3 and MEK inhibitor sensitivities observed in those cells.

5.2.2 Differential drug sensitivities in primary cells

We next performed DSRT on primary BM MNCs from AML patients and healthy donors to learn more about the drug sensitivities in *NUP98-NSD1*$^{+}$/*FLT3*-ITD^{+} patients (Figure 9). The index patient was tested with 171 drugs and other three patients with 306 drugs. By analysing commonly tested drugs between patients and healthy donors, we observed that 58% (99/171) of drugs were more effective in patients than in healthy cells, 30% (51/171) had no response (DSS = 0), and 12% (21/171) had negative median DSS difference suggesting drug resistance.

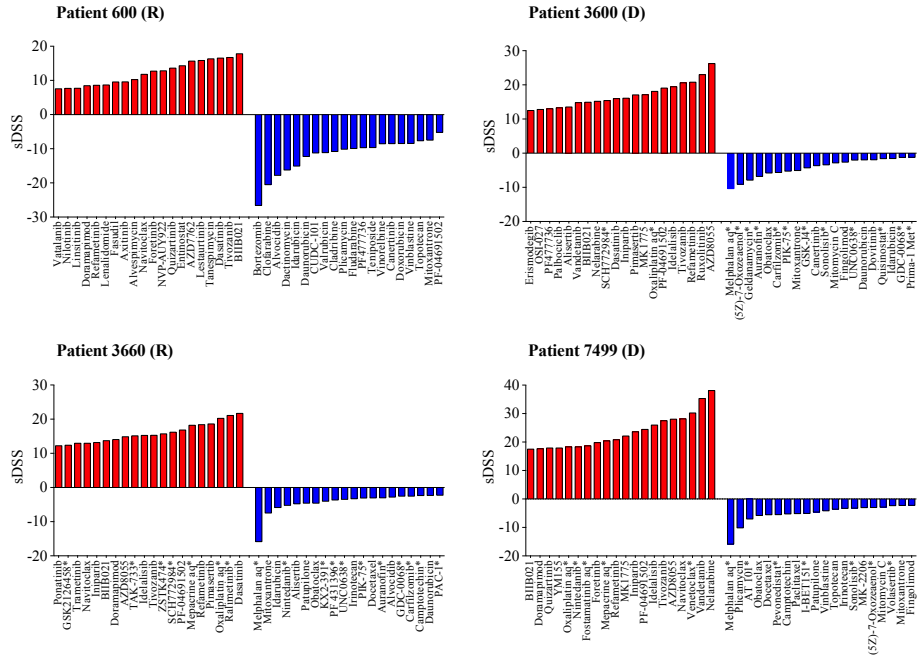

Figure 9 Waterfall plots showing differential drug sensitivities in AML patients with *NUP98-NSD1* and *FLT3*-ITD. Horizontal bars highlight the 20 most and least effective drugs in four patients compared to median DSS of ten healthy donors. The drugs marked with an asterisk were not tested in the index patient. Two samples were collected at diagnosis (D) and two at relapse (R).

As shown in Table 6, 15% (25/171) of the tested drugs had significant ($P < 0.01$) median DSS difference between *NUP98-NSD1*$^+$/*FLT3*-ITD$^+$ AML patients and healthy donors (Table 1). The drugs included one probe, 19 investigational drugs, and five clinically approved drugs. Of the approved drugs, dasatinib had the highest specificity toward *NUP98-NSD1*$^+$/*FLT3*-ITD$^+$ cells (median DSS difference: 16.3) and the lowest mean IC_{50} (2.2 nM, 95% CI -1.4-5.8 nM). Only one drug (mitoxantrone) had negative DSS difference, however, several topoisomerase inhibitors had negative DSS difference indicating that *NUP98-NSD1*$^+$/*FLT3*-ITD$^+$ cells may be intrinsically resistant to this class of drugs.

Table 6. *The most differentially sensitive drugs between NUP98-NSD1*$^+$*/FLT3-ITD*$^+$ *AML patients and healthy controls (P < 0.01).*

DRUG NAME	MOLECULAR TARGET	STATUS	DSS MEDIAN DIFFERENCE	95%CI DSS (PATIENTS)	95%CI DSS (HEALTHY)	P VALUE
AZD8055	mTOR	Phase 1	20.5	(4.1, 38.9)	(1.1, 5.6)	0.004
REFAMETINIB	MEK1/2	Phase 1/2	19.6	(8.3, 26.8)	(0.0, 3.0)	0.002
TIVOZANIB	FLT3, VEGFR1-3, c-Kit, PDGFR	Phase 2	18.7	(11.5, 28.9)	(-0.3, 6.4)	0.001
IDELALISIB	PI3K, p110 δ-selective	Phase 3	17.4	(4.4, 32.5)	(1.1, 3.9)	0.004
PIMASERTIB	MEK1/2	Phase 2	17.1	(6.2, 24.7)	(0.3, 3.2)	0.002
DASATINIB	ABL1, c-KIT, SRC, LCK	Approved	16.3	(11.9, 23.2)	(-0.2, 7.1)	0.003
BIIB021	HSP90	Phase 2	16.2	(21.5, 27.8)	(7.0, 9.8)	0.002
NAVITOCLAX	BCL-2, BCL-xL, BCL-w, BCL2A1, MCL-1	Phase 2	12.4	(12.1, 41.1)	(9.6, 12.8)	0.002
LESTAURTINIB	FLT3, JAK2, TrkA-C	Phase 3	11.6	(9.6, 20.4)	(3.0, 6.6)	0.002
DORAMAPIMOD	pan-p38 MAPK, c-RAF, FYN, LCK	Phase 1/2	11.3	(4.9, 19.9)	(0.0, 3.6)	0.001
FORETINIB	MET, VEGFR2	Phase 2	10.8	(3.1, 25.8)	(2.9, 5.0)	0.004
AZD7762	Chk1	Probe	10.3	(7.5, 24.3)	(5.3, 8.3)	0.008
LUMINESPIB	HSP90	Phase 2	10.2	(21.4, 26.7)	(11.5, 15.8)	0.002
OSI-027	mTOR	Phase 1	9.9	(6.7, 18.7)	(0.6, 4.2)	0.002
LINSITINIB	IGF1R, IR	Phase 2	9.5	(3.2, 17.0)	(0.6, 3.3)	0.004
TANESPIMYCIN	HSP90	Phase 2	9.2	(12.6, 24.3)	(7.0, 9.6)	0.002
EVEROLIMUS	mTOR	Approved	8.2	(2.8, 14.0)	(-0.5, 2.6)	0.002
BELINOSTAT	HDAC	Phase 2	7.2	(20.9, 29.3)	(15.3, 18.3)	0.002
AXITINIB	VEGFR, PDGFR, KIT	Approved	5.2	(2.6, 14.9)	(1.6, 4.3)	0.004
DANUSERTIB	Aurora kinase A-C, Abl, c-RET, LCK	Phase 2	4.9	(10.6, 13.5)	(4.7, 8.1)	0.002
ENTINOSTAT	HDAC	Phase 2	4.9	(2.5, 20.4)	(3.9, 5.8)	0.004
PICTILISIB	PI3Kα/δ	Phase 2	4.5	(8.9, 16.7)	(6.5, 8.5)	0.002
PANOBINOSTAT	HDAC	Phase 3	4.2	(22.9, 30.3)	(19.4, 22.6)	0.002
VORINOSTAT	HDAC	Approved	4.2	(9.0, 15.4)	(5.8, 9.0)	0.002
MITOXANTRONE	Topoisomerase II	Approved	-6.3	(-2.0, 5.8)	(5.9, 8.6)	0.008

To study *NUP98-NSD1*$^+$/*FLT3*-ITD$^+$ specificity further, we compared median DSSs between *NUP98-NSD1*$^+$/*FLT3*-ITD$^+$ (n = 4) and *NUP98-NSD1*$^-$/*FLT3*-ITD$^+$ (n = 9) BM MNC samples. Three drugs, namely dasatinib (P = 0.03), belinostat (P = 0.02), and tivozanib (P = 0.03), had significantly higher sensitivity in the *NUP98-NSD1*$^+$/*FLT3*-ITD$^+$ samples compared to *NUP98-NSD1*$^-$/*FLT3*-ITD$^+$ samples, while topoisomerase II inhibitor mitoxantrone had significantly lower sensitivity (Figure 10). We also evaluated the impact of blast percentage on differential drug sensitivities since *NUP98* rearrangements have been shown to

affect CD34+ progenitor cells in myeloid and lymphoid leukemias (138). We found that dasatinib sensitivity correlates positively (R = 0.800) with BM blast percentage in the *NUP98-NSD1*$^{+}$*/FLT3*-ITD^{+} BM MNCs, but not in *NUP98-NSD1*$^{-}$*/FLT3*-ITD^{+} cells (R = 0.25) (Figure 11). Based on these results, dasatinib was selected for combinatorial drug synergy screening experiments.

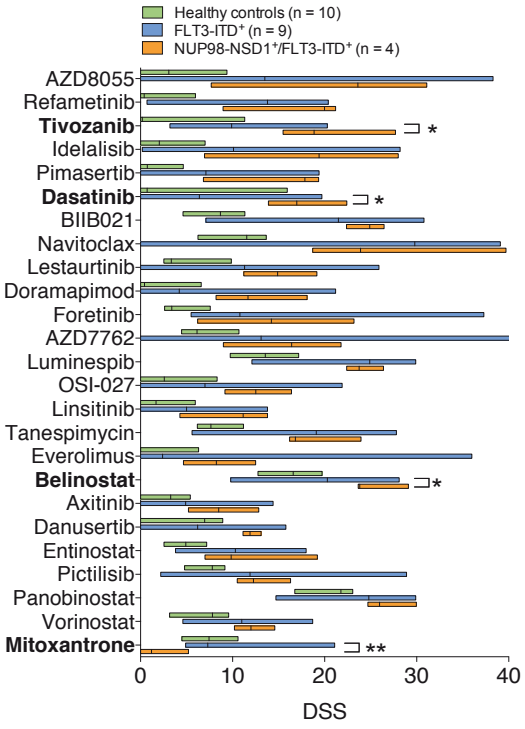

Figure 10 The graph shows comparison of *ex vivo* drug sensitivities of top candidate compounds in healthy controls, *FLT3*-ITD^{+} AML BM MNCs and *NUP98-NSD1*$^{+}$*/FLT3*-ITD^{+} BM MNCs. Significant differences are denoted with an asterisk (*, $P < 0.05$; **, $P < 0.01$).

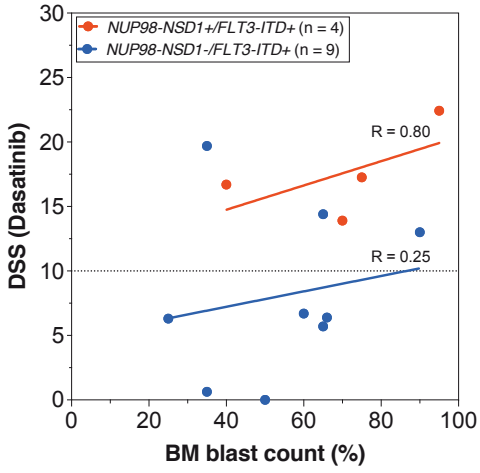

Figure 11 Dasatinib sensitivity correlates with malignant cell percentage. The graph illustrates *ex vivo* dasatinib sensitivity (Y-axis) and relative frequency of BM blast cells in AML patients at the time of BM sampling. Correlation coefficients (R-score) are shown above the linear regression line.

5.2.3 Combinatorial drug screening

Pilot combinatorial drug screening experiments were done with experimental mouse cell lines. By testing 70 compounds ± 100nM dasatinib, we observed that multikinase inhibitor dasatinib improves FLT3 and MEK inhibitor efficacies significantly in the *NUP98-NSD1*$^{+}$/*FLT3*-ITD^{+} cells (Figure 12), but not in other cell types.

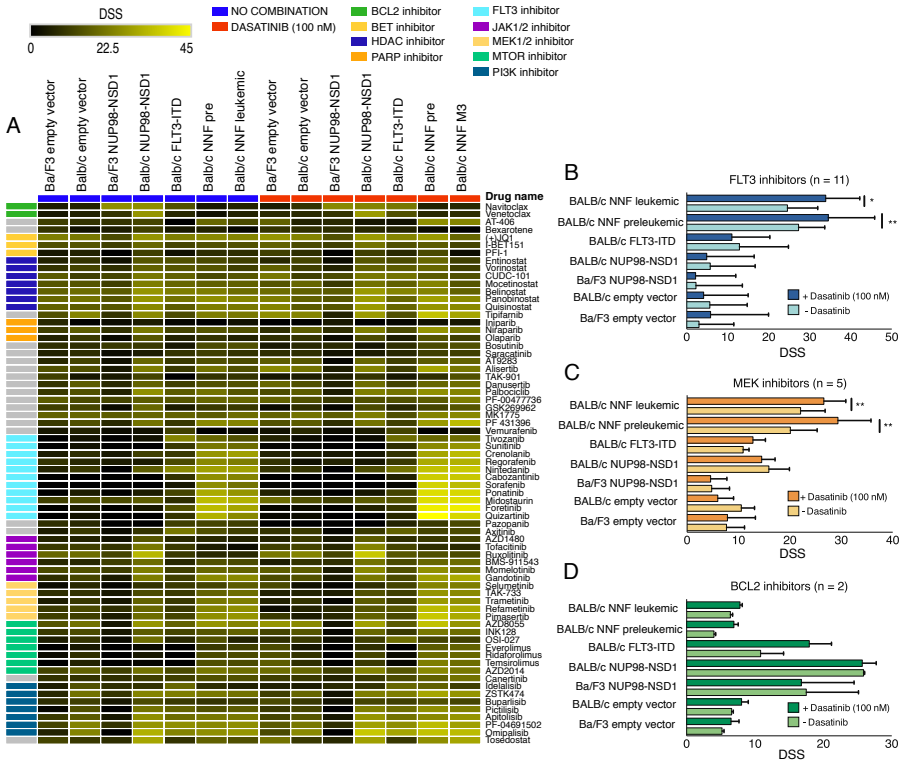

Figure 12 Pilot combination screen. (A) The heatmap shows DSS of 70 drugs ± 100 nM dasatinib in experimental cell lines. (B-C) The histograms show mean DSS with 95% CI. Significant differences were found in dual NUP98-NSD1^{+}/FLT3-ITD^{+} BALB/c cells for FLT3 and MEK inhibitors (*, P =0.02; **, P < 0.01). (D) NUP98-NSD1^{+} cells had high BCL-2 inhibitor sensitivity, however, 100 nM dasatinib increased response only modestly.

To investigate potentially synergistic drug pairs further, we selected eleven drug pairs from the pilot screen for more systematic analysis with 8×8 and 6×6 pairwise matrices. Notably, we discovered that multikinase inhibitor dasatinib

shows the strongest synergistic interactions with pan-BCL-2 inhibitor navitoclax in *NUP98-NSD1*$^{+}$/*FLT3*-ITD^{+} primary patient cells and leukemic dual positive mouse cells. As shown in Figure 13, the most synergistic area scores in patient 600, 7499, and leukemic BALB/c cells were 14.0, 6.1, and 9.4, respectively. In both patients, the highest *ex vivo* synergy was observed at an area where 0.1 nM dasatinib was combined with 30-300 nM navitoclax (56-62% inhibition). The highest synergy score was observed in leukemic mouse cells when 3 nM dasatinib was combined with 300 nM navitoclax.

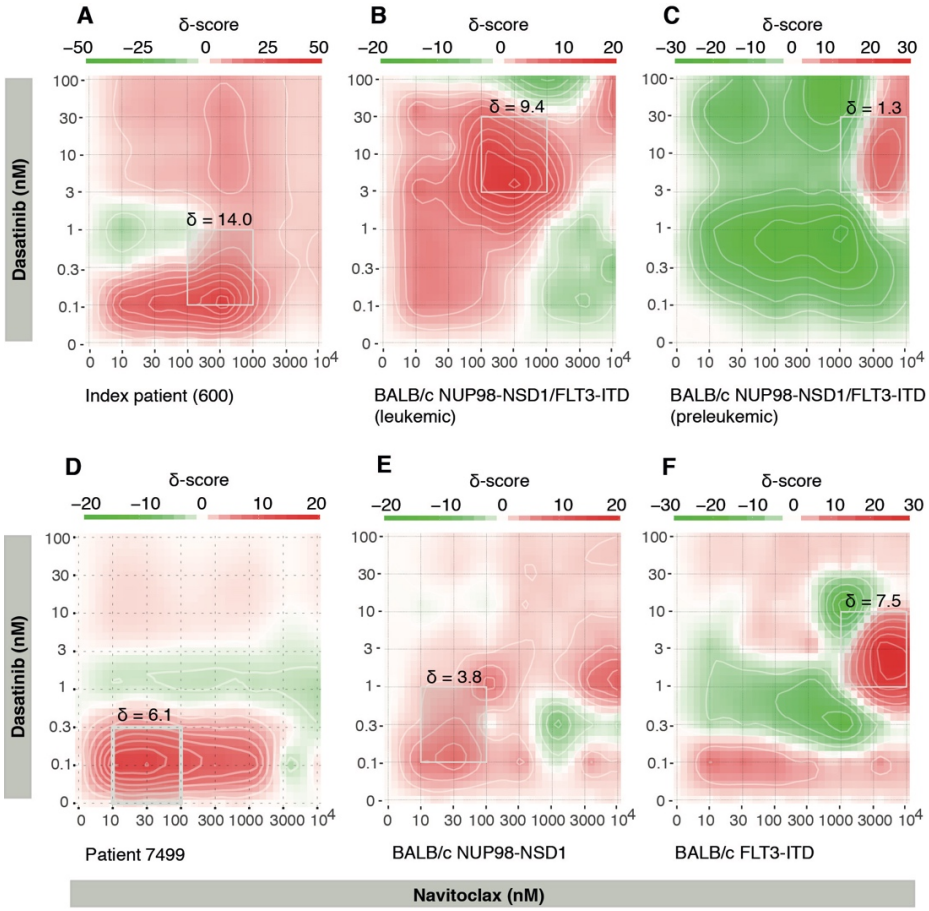

Figure 13 Synergy plots. The 2-dimensional contour plots show areas of synergy (red) and antagonism (green) in primary patient cells and experimental cell lines when tested with different concentrations of dasatinib and navitoclax. The white squares indicate the most synergistic area.

5.2.4 Gene expression analysis

To investigate biological mechanisms underlying observed drug sensitivities, we performed RNA-Seq to patient-derived BM MNCs, BM CD34+ cells from healthy controls, and experimental BALB/c BM cells. Initially, we evaluated the expression of *HOX*-cluster genes since overexpression of these genes is a known feature of *NUP98-NSD1*$^{+}$ AML (116, 124, 129). In consonance with previous studies, we found that *NUP98-NSD1*$^{+}$/*FLT3*-ITD^{+} patients overexpress *HOX-A9, HOX-A10, HOX-B3, -B4, -B5, -B6,* and *-B7* genes relative to normal CD34+ cells. More importantly, by sequencing experimental BALB/c cells, we confirmed the findings of Wang *et al* who reported earlier that NUP98-NSD1 alone induces constitutive expression of many *HOX* cluster genes (129). As expected, FLT3-ITD alone did not induce *HOX* genes (Figure 14 A-B).

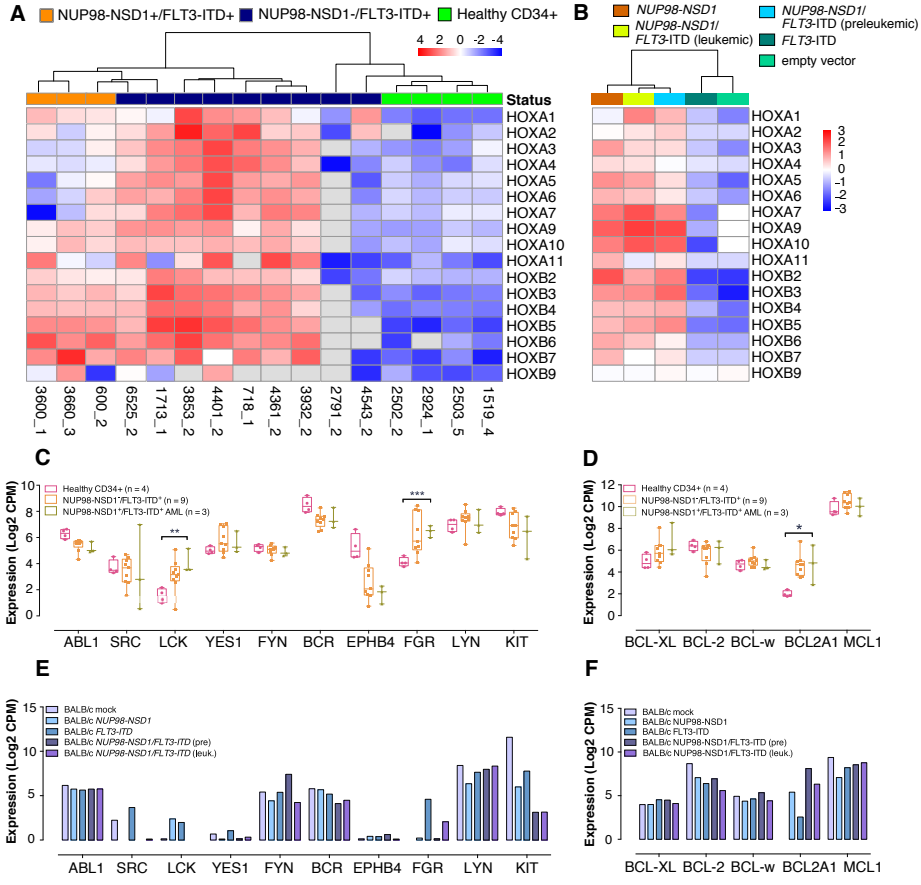

Figure 14 Transcriptome analysis. Unsupervised hierarchical clustering of *HOX-AB* cluster genes was done using 16 primary BM samples (A) and five experimental BALB/c cell lines (B) based on mean centered and log2 transformed expression values (Log2 CPM) using Euclidean distance with complete linkage method. Heatmaps were drawn with R package pheatmap (1.0.8). (C-F) The lower panels show the RNA-level expression of dasatinib and navitoclax targets in human and mouse samples. The asterisks define levels of statistical significance (*, P = 0.028; **, P = 0.006; ***, P = 0.0006).

We next compared the log2-transformed (Log2 CPM) expression levels of various dasatinib and navitoclax target proteins relative to healthy CD34+ BM cells. Although number of dissimilarities were observed, *LCK (P = 0.005)*, *FGR* (*P < 0.001*), and *BCL2A1* (*P = 0.028*) were the only significantly overexpressed genes (Figure 11C-D). Statistical analyses could not be performed on experimental BALB/c cells; however, data strongly suggests that NUP98-NSD1 alone may induce *BCL2A1* expression (Figure 14F). The data shows that BCL-2 inhibitor resistant leukemic *NUP98-NSD1*$^{+}$*/FLT3*-ITD^{+} BALB/c cells have the highest expression of anti-apoptotic *MCL-1,* although connection between BCL-2 inhibitor resistance and increased *MCL-1* expression remains undetermined. To learn more about the potential causes of high dasatinib sensitivity, we evaluated phosphorylation of several SRC family kinases from phosphokinase antibody array analysis previously performed on index patient (149). Intriguingly, phosphorylation of LCK, FYN, and LYN was increased in *NUP98-NSD1*$^{+}$*/FLT3*-ITD^{+} index patient compared to healthy controls in samples collected at three different time-points (Figure 15).

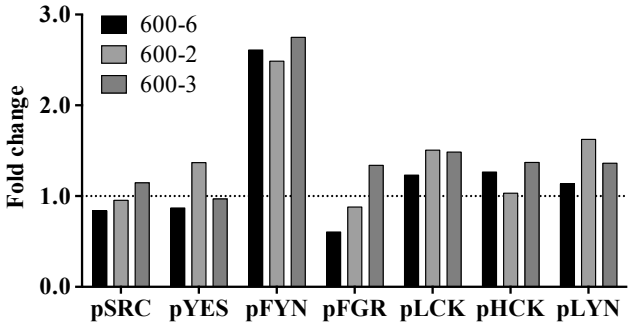

Figure 15 Phosphokinase antibody array results. The graph shows phosphorylation status of several SRC family kinases in three samples from the index's patient relative to healthy control.

6 DISCUSSION

6.1 Molecular monitoring of *NUP98-NSD1* (I)

The aim of study (I) was to discover whether previously unknown *NUP98-NSD1* fusion transcripts are expressed in AML patients with cytogenetically silent t(5;11) translocation and to learn whether current molecular monitoring methods for *NUP98-NSD1* need improvement. The questions were based on previous work, which had discovered two chimeric *NUP98-NSD1* transcripts from an adult refractory anemia (RAEB) patient with excess blasts (11). RAEB frequently proceeds to AML (162), so we anticipated that novel *NUP98-NSD1* transcripts may exist in AML as well. Another reason prompting us to study this particular aberration was that translocation t(5;11) is undetectable by routine cytogenetic methods (G-banding) due to its cryptic nature and subtelomeric localization. The detection of t(5;11) therefore relies on robustly designed molecular screening methods.

By utilizing standard molecular cloning and NGS methods, we generated evidence showing that post-transcriptional processing of *NUP98-NSD1* produces three alternative mRNA transcripts in AML (140). From these transcripts, we found two fusion junctions (juxtaposing *NUP98* exon 11/12 to *NSD1* exon 6), alternative 5' donor site of *NUP98* exon 7 and differentially spliced *NSD1* exon 7. We discovered that the previously unknown intragenic splice events involving *NUP98* exon 7 and *NSD1* exon 7 were present in healthy controls (N = 2) and patients without *NUP98-NSD1* (N = 10). This finding suggest that these events are normal post-transcriptional RNA modifications of wild type genes, which retain splicing activity upon acquisition of the t(5;11) translocation.

With sequential samples available from two patients, we found that *NUP98-NSD1*$^{+}$ fusion was present at relapse and chemorefractory stage (Figure 7A). The finding is consistent with a study describing *NUP98-NSD1* as a clonally stable founder alteration and notion that its increasing expression correlates with hematological relapse (116, 122). Consistently, Ostronoff *et al* has demonstrated association between *NUP98-NSD1* and chemoresistance by showing that most *NUP98-NSD1*$^{+}$ AML patients remain positive for the fusion at the end of first cycle of induction chemotherapy leading to high-rate of induction failure (120).

These studies confirm the role of *NUP98-NSD1* as a clinically relevant marker, not only for prognostication, but also for determining treatment efficacy and presence of minimal residual disease.

The co-expression of two alternative *NUP98-NSD1* transcripts (*NUP98* exon 11/12 to *NSD1* exon 6) detected in our study were present in all three *NUP98-NSD1*$^{+}$ study patients. In a follow-up analysis of two similar patients (data not shown) from TCGA AML cohort (4), however, the transcript joining *NUP98* exon 11 and *NSD1* exon 6 was not found. We think that the RNA-Seq coverage in the TCGA analysis may have been too low to expose supporting reads for the less frequent transcript or that there is heterogeneity in the *NUP98-NSD1* transcript levels between patients. The latter idea is supported by Shiba *et al* who identified sole expression of *NUP98* exon 11 and *NSD1* exon 6 fusion from a *NUP98-NSD1*-like pediatric AML patient (124). In favor of both ideas, a recent study by Audemard *et al* repeated our findings and reported co-expression of two in-frame *NUP98-NSD1* transcripts from 6 AML patients. Intriguingly, in their analysis one patient expressed only the well-known fusion between *NUP98* exon 12 and *NSD1* exon 6 (163). Taken together, results from available studies imply that in spite of few outliers, majority of AML patients with *NUP98-NSD1* co-express at least two in-frame *NUP98-NSD1* transcripts (*NUP98* exon 11/12 to *NSD1* exon 6). We conclude that adjustment of oligonucleotide probes to detect both fusion junctions (*NUP98* exon 11/12 to *NSD1* exon 6) is important to ensure all patients with *NUP98-NSD1* are appropriately identified during pre-diagnostic screening. This adjustment will not only improve the accuracy of MRD quantification at post-treatment follow-up, but will also teach us whether frequencies of the two alternative *NUP98-NSD1* transcripts may fluctuate in response to treatment and play role in drug resistance.

Few limitations to study I need to be acknowledged. Firstly, the presented results should be confirmed in larger series of *NUP98-NSD1*$^{+}$ AML patients in order to draw stronger conclusions. Our analysis was limited to three adult patients due to infrequency of *NUP98-NSD1* fusion gene in AML and low overall incidence of AML in Finland. In a study published in 2012, *NUP98-NSD1* was identified from roughly 2% and 16% of adult and pediatric CN-AML patients, respectively (116). The relative frequency of *NUP98-NSD1* in Finnish population has not been systematically analysed. Based on the observed frequencies in other countries, our findings may have more importance for the management of pediatric rather than

adult AML patients. Secondly, we did not perform mechanistic studies to evaluate whether the identified in-frame *NUP98-NSD1* transcripts may convey different leukemogenic functions. Based on *in silico* analysis of structural domains (Figure 5B), the differences are expected to be minimal and limited to three FG repeats located in *NUP98* exons 7 and exon 12. Other than disparities in FG repeat count, all functional domains remained consistent between the two in-frame transcripts. We envision that on-going work at John Hopkins University with the plasmids we generated will shed light on functional differences between the two *NUP98-NSD1* transcripts. Thirdly, our RNA-Seq analysis identified additional anomalies, which could not be validated by cloning and Sanger sequencing. These anomalies included single read for RNA joining *NUP98* exon 6 to *NSD1* exon 12 and five reads to RNA joining *NUP98* exon 8 to *NSD1* exon 11. The analysis also revealed potential low-level transcripts joining *NUP98* exon 11 to *NSD1* exon 17 and exon 21. Whether these variants are real or artefacts remain to be determined. Based on the observation, however, we acknowledge that additional, currently unknown *NUP98-NSD1* transcripts may be generated in patients with t(5;11) translocation.

Additionally, it remains unclear whether the two in-frame *NUP98-NSD1* transcripts or their distribution may affect therapeutic responses and hematological parameters. Based on evidence from *BCR-ABL1* fusion gene, this may be relevant question. A study by Adler *et al* revealed equal distribution of coexpressed b2a2 (e13a2) and b3a2 (e14a2) transcripts between genders, whereas the sole expression of either form showed uneven distribution. In the same study, higher platelet count in conjunction with leukocytosis was more frequent in patients expressing the b3a2 transcript (164). Furthermore, two independent studies have shown that uneven distribution of b2a2 and b3a2 transcripts impacts molecular response to imatinib (165, 166). Analogous to *BCR-ABL1*, alternative *NUP98-NSD1* transcripts could distribute unevenly between population subgroups or influence distinct hematological parameters and therapy. Future study with a larger cohort of *NUP98-NSD1*$^{+}$ patients, such as the COG trial cohort (N = 32) or the French pediatric cohort (N = 17) of *NUP98-NSD1*$^{+}$ pediatric AML patients (120, 126), should explore the *NUP98-NSD1* transcripts further for revealing transcript distributions as well as their therapeutic implications (should patient material be available).

6.2 Therapeutic targeting of *NUP98-NSD1*$^{+}$ *AML* (II)

In study II, our aim was to discover novel treatment options for high-risk AML patients with concomitant *NUP98-NSD1* fusion gene and *FLT3*-ITD using high-throughput drug screening and NGS methods. The main motivation for starting the project was that majority of *NUP98-NSD1*$^{+}$/*FLT3*-ITD^{+} AML patients never achieve CR (144) and those that do, eventually become chemoresistant (120). Due to chemoresistance and high rate of relapse (116), it is crucial to find novel therapeutics for this patient subset. Using state-of-the-art technologies, we acquired evidence indicating that *NUP98-NSD1*$^{+}$/*FLT3*-ITD^{+} patients may benefit from combinatorial treatment with multikinase inhibitor dasatinib and pan-BCL-2 inhibitor navitoclax. Dasatinib and navitoclax targeted *NUP98-NSD1*$^{+}$/*FLT3*-ITD^{+} BM MNCs selectively as single agents and synergistically in combination (Figure 13). Additional drug classes with selective efficacy against *NUP98-NSD1*$^{+}$/*FLT3*-ITD^{+} BM MNCs included HDAC inhibitors, FLT3 inhibitors, and inhibitors of MAP kinase and PI3K/AKT pathways (Table 6).

In the DSRT assay, dasatinib was the most selective drug for *NUP98-NSD1*$^{+}$/*FLT3*-ITD^{+} BM MNCs. Dasatinib (BMS-354825) is a multikinase inhibitor targeting BCR-ABL, SRC family (SRC, LCK, FGR, YES, FYN), c-KIT, EPHA2, and PDGFRβ. It has FDA approval for the treatment of CML and ALL, and is currently being evaluated in a phase III clinical trial with and without chemotherapy for adult core binding factor AML (NCT02013648). The phase III trial was initiated following a successful phase Ib/IIa study (167). Consistent with known drug targets, we discovered that dasatinib sensitivity in *NUP98-NSD1*$^{+}$/*FLT3*-ITD^{+} BM MNCs may result from increased expression of *LCK* or *FGR* genes (Figure 14). Out of the two genes, *LCK* appears to be most relevant as we found three LCK targeting drugs (dasatinib, doramapimod, danusertib) among the top hits (Table 6). The relevancy of LCK in *NUP98-NSD1*-driven leukemogenesis is also supported by our expression analysis on mouse cells, which showed that NUP98-NSD1 alone may induce *LCK* expression (Figure 14E). Interestingly, NUP98-NSD1 and LCK have both been shown to cooperate with FLT3-ITD in cellular transformation (146, 168). Therefore, hypothetical connection between NUP98-NSD1 and LCK appears highly interesting and worth studying in more detail.

To date, no cancer pharmacopeia-wide drug screening studies have been done on *NUP98-NSD1*$^{+}$/*FLT3*-ITD^{+} AML samples. Therefore, we are limited to interpreting our findings in the light of mechanistic studies performed on *NUP98* rearrangements and structurally similar *MLL* rearrangements (169). A common theme, which clearly emerges is that epigenetic dysregulation may lead to highly selective BCL-2 inhibitor sensitivities in *NUP98-NSD1*$^{+}$ AML cells. Fairly recent work by Benito *et al* found BCL-2 to be a direct transcriptional target of MLL-AF4. They showed that MLL-AF4 upregulates BCL-2 by DOT1L-mediated H3K79 methylation activity, which leads to high BCL-2 inhibitor (venetoclax) sensitivity (170). Congruently, abnormal H3K79 and H3K36 methylation activities have been shown to be vital for *NUP98-NSD1*-dependent leukemogenesis as well (129, 134). Another line of evidence linking aberrant methylation activities of NUP98-NSD1 to antiapoptotic BCL-2 family members relates to activation of NF-κB. Studies have demonstrated that, through lysine methylation, NSD1 activates p65 subunit of NF-κB (171), which directly controls BCL2A1 expression (172). It remains unstudied whether this function of NSD1 is retained in the NUP98-NSD1 fusion. Since *BCL2A1* was the only significantly upregulated antiapoptotic BCL-2 family member in our study (Figure 14D), the scheme seems highly plausible. Based on the above-mentioned findings, we picture that the highly selective BCL-2 inhibitor responses observed in *NUP98-NSD1*$^{+}$/*FLT3*-ITD^{+} AML cells may arise as a result of NUP98-NSD1-mediated aberrant histone methylation that activate antiapoptotic BCL-2 family members such as BCL2A1. Future studies should study the potential connection between aberrant lysine methylation and BCL-2 inhibitor sensitivity in AML patients with *NUP98-NSD1* fusion gene as well as structurally similar *NUP98* rearrangements. Moreover, potential efficacy of BCL-2 inhibitor venetoclax should be evaluated in prospective studies as navitoclax is currently unavailable for clinical use.

Curiously, we observed striking differences in BCL-2 inhibitor responses between *NUP98-NSD1*$^{+}$/*FLT3*-ITD^{+} patient cells and mouse progenitor cells co-transduced with *NUP98-NSD1* and *FLT3*-ITD indicating our mouse model does not fully reflect the molecular complexities present in human cells. The patient cells were highly sensitive to BCL-2 inhibitors similar to mouse cells transduced with *NUP98-NSD1* alone, while the leukemic dual positive mouse cells were BCL-2 inhibitor resistant (Figure 8). Based on these discrepancies, additional aspects to BCL-2 inhibitor responses in *NUP98-NSD1*$^{+}$/*FLT3*-ITD^{+} BM MNCs need to be considered. One relevant aspect could be *WT1* mutations. Exome sequencing

performed on two of the study patients revealed hotspot mutations in the DNA-binding domain of *WT1* gene. Recent work has shown that up to 45% of *NUP98-NSD1*$^{+}$ AML patients have *WT1* mutations (116, 120) and that patients with *WT1* mutations have significantly increased sensitivity to BCL-2 inhibitor venetoclax (173). It remains unclear how *WT1* mutations mediate increased BCL-2 inhibitor sensitivity. Based on Morrison *et al*, WT1 mutant proteins may fail to activate programmed apoptosis by not being able to induce proapoptotic BAK expression (174). This inability may tip the balance between pro-and antiapoptotic BCL-2 members to favor antiapoptotic proteins. To follow-up on these responses, it would be relevant to develop a triple positive (*NUP98-NSD1*$^{+}$/*FLT3*-ITD^{+}/*WT1*$^{+}$) mouse cell line and evaluate whether *WT1* mutation resensitizes BCL-2 inhibitor resistant leukemic *NUP98-NSD1*$^{+}$/*FLT3*-ITD^{+} mouse cells to BCL-2 inhibitors. Moreover, this model would inform how WT1 mutant protein impact expression of pro- and antiapoptotic BCL-2 proteins in cells coexpressing NUP98-NSD1 and FLT3-ITD.

Four HDAC inhibitors (belinostat, entinostat, panobinostat, and vorinostat) were among the 24 most selective compounds targeting *NUP98-NSD1*$^{+}$/*FLT3*-ITD^{+} BM MNCs. Intriguingly, Kasper *et al* demonstrated already two decades ago that *NUP98* rearrangement (*NUP98-HOXA9*) recruits CREB-binding protein (CBP)/p300 histone acetyltransferase, which physically interacts with FG repeat rich areas of NUP98 (175). Later work by Wang and colleagues showed with *NUP98-NSD1*$^{+}$ mouse progenitors that CBP/p300 mediated acetylation of H3/H4 around *HoxA7-A9* locus is a key step (together with H3K36 methylation) in the prevention of EZH2-mediated transcriptional silencing of *HOX* cluster genes (129). Regardless of earlier findings, it remains unclear whether HDAC inhibitors may reverse aberrant histone acetylation at *HOXA7-A9* locus and silence constitutively active *HOX* genes in *NUP98-NSD1*$^{+}$ leukemic cells. Based on the high *ex vivo* efficacy of HDAC inhibitors observed in our study, future studies should explore the functional impact of these inhibitors further in the context of *NUP98-NSD1*$^{+}$/*FLT3*-ITD^{+} AML.

Another interesting feature of our data was that dual positive transgenic BALB/c BM cells had significantly higher sensitivity to FLT3 inhibitors (n = 11) compared to cells expressing FLT3-ITD alone (Figure 8). This seems to confirm the previously proposed functional cooperation between NUP98-NSD1 and FLT3-ITD in AML induction (146). In line with the findings of Thanasopoulou *et al*,

functional cooperation between NUP98-HOXD13 and FLT3-ITD, as well as between MLL-AF9 and FLT3-ITD in AML induction have been reported (176, 177). It is therefore likely that our findings regarding FLT3 inhibitors could be expanded to other functionally cooperative mutation pairs. Regardless of the promising FLT3 inhibitor efficacies observed *in vitro*, the *ex vivo* efficacies were not as encouraging. Only two (2/6) non-specific FLT3 inhibitors (tivozanib, lestaurtinib) reached statistically significant responses in *NUP98-NSD1*$^+$/*FLT3*-ITD$^+$ AML cells and were less effective than multikinase inhibitor dasatinib. Similar responses have been observed in the clinic between these compounds. The differences in FLT3 inhibitor efficacies between mouse cell lines and patient cells may result from differences in FLT3-ITD expression levels. Notably, retroviral transduction frequently results in super-physiologic levels of transgene expression (178). In our study, we did not compare relative FLT3-ITD expression levels between patient cells and mouse cell lines to learn if FLT3 inhibitor sensitivity differences are related to expression-levels. According to Pratz *et al*, FLT3-mutational load predicts responses to FLT3 inhibitors, particularly in relapse samples (100). In their work, highest FLT3 inhibitor sensitivities were found in patient samples with high mutant allelic burden (above 50%). In our study, *NUP98-NSD1*$^+$/*FLT3*-ITD$^+$ AML samples had low (17-40%) *FLT3* allelic burden (Table 4), which could explain the low *ex vivo* FLT3 inhibitor sensitivities. Accordingly, future work should evaluate the efficacy of FLT3 inhibitors further in respect to relapsed *NUP98-NSD1*$^+$ AML patients with high *FLT3*-ITD mutation load.

Few limitations to our study need to be acknowledged. Firstly, our findings should be confirmed in larger series of *NUP98-NSD1*$^+$/*FLT3*-ITD$^+$ AML patients since only four *NUP98-NSD1*$^+$ AML patients were tested. We compensated for this limitation by including two separate control groups (healthy samples and AML patients with *FLT3*-ITD) and by testing experimental BALB/c cell lines. Secondly, drug sensitivity assessment should have been performed using fresh, treatment naïve BM MNCs, with equal number of drugs. Two of our samples were collected after induction therapy and two were tested after cryopreservation. Three BM MNC samples were tested with 306 drugs and one sample with 171 drugs. Finally, molecular profiling experiments should have been performed to all *NUP98-NSD1*$^+$/*FLT3*-ITD$^+$ study patients. In our study, RNA-Seq was executed to 3 out of 4 patients and exome sequencing to 2 out of 4. Had this data been available, we could be more certain about the deregulated genes associated with

NUP98-NSD1-driven AML, their impact on drug responses, and presence of additional comutations. In summary, the results presented in study II improves the current understanding of potentially efficient treatments for AML patients with concomitant *NUP98-NSD1* and *FLT3*-ITD. These data provide a reference point for future studies regarding this topic as well as proof-of-concept clinical studies.

7 CONCLUSIONS

In this thesis, we used RNA-Seq and standard molecular biology methods to characterize alternative *NUP98-NSD1* fusion transcripts from AML patients with cryptic t(5;11)(q35;p15.4) translocation. Moreover, we investigated novel therapeutic opportunities for patients with *NUP98-NSD1* and concomitant *FLT3*-ITD alteration using high-throughput DSRT and NGS. The primary conclusions from these studies are as follows:

1. Post-transcriptional modification generates at least three *NUP98-NSD1* mRNA transcripts from *NUP98-NSD1* gene fusion in AML patients with t(5;11). Distinctive features within the three transcripts include two alternative fusion junctions juxtaposing either *NUP98* exon 11 or 12 to *NSD1* exon 7, alternative 5' donor site at *NUP98* exon 7, and skipping of *NSD1* exon 7. Based on these findings, previously unknown transcript joining *NUP98* exon 11 to *NSD1* exon 7 should be considered in the design of molecular monitoring tests for this prognostically significant aberration.

2. Multikinase inhibitor dasatinib and pan-BCL-2 inhibitor navitoclax target *NUP98-NSD1*$^+$/*FLT3*-ITD$^+$ AML patient cells selectively as single agents and synergistically in combination. *NUP98-NSD1*$^+$/*FLT3*-ITD$^+$ BM MNCs are highly resistant to conventional chemotherapeutics such as type II topoisomerase inhibitors.

8 ACKNOWLEDGEMENTS

The work presented in this thesis was completed at the Institute for Molecular Medicine Finland (FIMM), University of Helsinki. I warmly thank the founding director of FIMM Professor Olli Kallioniemi, the interim director Professor Jaakko Kaprio, and the current director Professor Mark Daly for developing the state-of-the-art research infrastructure and inspiring working environment at FIMM.

I am forever grateful to my primary supervisor Doctor Caroline Heckman for giving me the opportunity to carry out PhD studies at FIMM. I thank her for all the guidance and support during the past 6 ½ years. It has been a priviledge to work in an open and relaxed working atmosphere that fosters creativity and encourages us to follow our own research interests. Caroline has given me plenty of freedom, but also significant amount of responsibilities to make me more independent as a researcher. I owe a great deal of thanks to my co-supervisor Professor Kimmo Porkka for his visionary leadership and opportunities to perform research in close collaboration with the hematology clinic at the Helsinki University Hospital. Under Kimmo's and Caroline's mentorship, I gained a first-hand view of groundbreaking translational cancer research and personalized medicine.

I thank my thesis committee members, Professor Minna Nyström and Professor Lauri Aaltonen for critically evaluating my progress and providing invaluable feedback during the meetings. Their encouragement and constructive criticism steered me in the right direction and created pressure to move things forward in a timely fashion. I wish to thank Docent Mervi Taskinen and Adjunct Professor Jorrit Enserink for carefully revising my dissertation and for their constructive criticism. I sincerely thank Associate Professor Linda Fogelstrand for accepting our invitation to be the opponent.

I acknowledge with thanks and deep gratitude my co-authors, Jesus, Angeliki, Ashwini, Mika, Alun, Bhagwan, Mamun, Maija, Tuija, Henrik, Samuli, Juerg, Kimmo, and Caroline, who devoted significant amount of their valuable time for the present work by performing experiments, providing research material, preparing figures, analysing complex sequencing and drug testing data, driving up

and down the English lanes of our manuscripts, and taking time to meet and discuss about research. This thesis work would not have been possible without such a multi-talented team of professionals with different expertise. I especially thank Doctor Mika Kontro for his contribution over the years, his positive energy, and for initiating the collaborative research project with Professor Juerg Schwaller's group.

I am grateful to collaborators Professor Jüerg Schwaller and Dr. Angeliki Thanasopoulou at the University Children's Hospital Basel for providing experimental cell lines. I thank Jüerg for providing the opportunity to visit his laboratory in 2015 and Angeliki for repeatedly sending me experimental samples. I am also obliged to Angeliki for her patience while teaching me new lab techniques during the 2-month lab visit. During that time, I learned several Greek words that still come handy at times. Moreover, I thank Professor Björn Tøre Gjertsen and Dr. Monica Hellesoy at the University of Bergen (Norway) for the on-going collaborative research.

I am obliged to thank the staff at the FIMM high-throughput biomedicine unit including Laura, Jani, Swapnil, Karoliina, Maria, Katja, Elina, Tanja, and Sergey for their help with drug screening assays. I am particularly thankful to Laura for preparing countless DSRT-plates and to Jani and Swapnil for their help with QC and data transformation.

I am pleased to have received financial support from Väre Foundation for Pediatric Cancer Research, Emil Aaltonen Foundation, Ida Montin Foundation, Finnish Hematology Association, Cancer Society of Finland, Integrative Life Sciences doctoral program (ILS), University of Helsinki, and FIMM. The salary support, personal grants and travel grants enabled me to work full-time and attend numerous conferences, courses, meetings, and workshops around the world. The contribution of these foundations and institutions has been highly important part of the training.

I sincerely thank all my colleagues at the Translational Research and Personalized Medicine Group at FIMM led by Doctor Caroline Heckman, including Samuli, Minna, Siv, Aino-Maija, Annukka, Cristina, Komal, Juho, Minxia, Joseph, Romika, Alina, Alun, Mamun, Heikki, Dimitrios, Ashwini, and Riikka for the great times we shared together in and out of the laboratory. I could not ask for

more helpful and friendly colleagues to work with. I acknowledge FIMM Unscientific Kaffee Klubben (FUK) members: Riku, Vesa, Teijo, Sami, Andrew, Lassi, Oscar, Risto, Heikki, and Pyry for our daily coffee breaks and unscientific discussions, which were highly entertaining and provided much needed break from work from time to time.

I am thankful for all of the patients and healthy donors who took part in this study. Without them it would not have been possible to perform this study.

Lastly, I want to thank my dear friends and relatives. I am especially thankful to my mom for her love and care. She has always been supportive and allowed me follow my dreams and ambitions. I warmly thank my friends Mika, Matti, Pekka, Henkka, Olli and "Känsä-group" for our friendship and joyful moments together over the years.

Helsinki, May 2019

Jarno Kivioja

9 REFERENCES

1. Deschler B, Lubbert M. Acute myeloid leukemia: epidemiology and etiology. Cancer. 2006;107(9):2099-107.
2. Schlenk RF, Döhner H. Hematology Am Soc Hematol Edu Program. 2013; 2013: 324-330: American Society of Hematology; 2013.
3. Ley TJ, Mardis ER, Ding L, Fulton B, McLellan MD, Chen K, et al. DNA sequencing of a cytogenetically normal acute myeloid leukaemia genome. Nature. 2008;456(7218):66-72.
4. Cancer Genome Atlas Research N, Ley TJ, Miller C, Ding L, Raphael BJ, Mungall AJ, et al. Genomic and epigenomic landscapes of adult de novo acute myeloid leukemia. N Engl J Med. 2013;368(22):2059-74.
5. Papaemmanuil E, Dohner H, Campbell PJ. Genomic Classification in Acute Myeloid Leukemia. N Engl J Med. 2016;375(9):900-1.
6. Chen Y, McGee J, Chen X, Doman TN, Gong X, Zhang Y, et al. Identification of druggable cancer driver genes amplified across TCGA datasets. PLoS One. 2014;9(5):e98293.
7. Gambacorti-Passerini C. Part I: Milestones in personalised medicine--imatinib. Lancet Oncol. 2008;9(6):600.
8. Huang ME, Ye YC, Chen SR, Chai JR, Lu JX, Zhoa L, et al. Use of all-trans retinoic acid in the treatment of acute promyelocytic leukemia. Blood. 1988;72(2):567-72.
9. Roberts PJ. Clinical use of crizotinib for the treatment of non-small cell lung cancer. Biologics. 2013;7:91-101.
10. Mertens F, Johansson B, Fioretos T, Mitelman F. The emerging complexity of gene fusions in cancer. Nat Rev Cancer. 2015;15(6):371-81.
11. La Starza R, Gorello P, Rosati R, Riezzo A, Veronese A, Ferrazzi E, et al. Cryptic insertion producing two NUP98/NSD1 chimeric transcripts in adult refractory anemia with an excess of blasts. Genes Chromosomes Cancer. 2004;41(4):395-9.
12. Velpeau A. Sur la resorption du puseat sur l'altération du sang dans les maladies clinique de persection nenemant. Premier observation Rev Med. 1827;2(216).
13. Bennett J. Two cases of hypertrophy of the spleen and liver, in which death took place from suppuration of blood. Edinburgh Med Surg J. 1845(64):413.
14. Virchow R. "Die Leukämie". In Virchow R. Gesammelte Abhandlungen zur Wissenschaftlichen Medizin. Frankfurt: Meidinger. 1856:190.
15. Ebstein W. Uber die acute Leukämie und Pseudoleukämie. Deutch Arch Klin Med. 1889;44(343).

16. Hoffman R. Hematology: Basic Principles and Practice (4th Ed). St Louis, Mo: Elsevier Churchill Livingstone. 2005:1074-5.
17. Ganzel C, Manola J, Douer D, Rowe JM, Fernandez HF, Paietta EM, et al. Extramedullary Disease in Adult Acute Myeloid Leukemia Is Common but Lacks Independent Significance: Analysis of Patients in ECOG-ACRIN Cancer Research Group Trials, 1980-2008. J Clin Oncol. 2016;34(29):3544-53.
18. Cribe AS, Steenhof M, Marcher CW, Petersen H, Frederiksen H, Friis LS. Extramedullary disease in patients with acute myeloid leukemia assessed by 18F-FDG PET. Eur J Haematol. 2013;90(4):273-8.
19. Byrd JC, Weiss RB, Arthur DC, Lawrence D, Baer MR, Davey F, et al. Extramedullary leukemia adversely affects hematologic complete remission rate and overall survival in patients with t(8;21)(q22;q22): results from Cancer and Leukemia Group B 8461. J Clin Oncol. 1997;15(2):466-75.
20. Hematopoiesis [Available from: http://tbl.med.yale.edu/myeloid_cells/reading.php.
21. Fircanis S, Merriam P, Khan N, Castillo JJ. The relation between cigarette smoking and risk of acute myeloid leukemia: an updated meta-analysis of epidemiological studies. Am J Hematol. 2014;89(8):E125-32.
22. Wong O, Harris F, Armstrong TW, Hua F. A hospital-based case-control study of acute myeloid leukemia in Shanghai: analysis of environmental and occupational risk factors by subtypes of the WHO classification. Chem Biol Interact. 2010;184(1-2):112-28.
23. Kuznetsova IS, Labutina EV, Hunter N. Radiation Risks of Leukemia, Lymphoma and Multiple Myeloma Incidence in the Mayak Cohort: 1948-2004. PLoS One. 2016;11(9):e0162710.
24. Kheifets LI, Afifi AA, Buffler PA, Zhang ZW, Matkin CC. Occupational electric and magnetic field exposure and leukemia. A meta-analysis. J Occup Environ Med. 1997;39(11):1074-91.
25. Cohen T, Creger WP. Acute myeloid leukemia following seven years of aplastic anemia induced by chloramphenicol. Am J Med. 1967;43(5):762-70.
26. Smith SM, Le Beau MM, Huo D, Karrison T, Sobecks RM, Anastasi J, et al. Clinical-cytogenetic associations in 306 patients with therapy-related myelodysplasia and myeloid leukemia: the University of Chicago series. Blood. 2003;102(1):43-52.
27. Czuczman MS, Emmanouilides C, Darif M, Witzig TE, Gordon LI, Revell S, et al. Treatment-related myelodysplastic syndrome and acute myelogenous leukemia in patients treated with ibritumomab tiuxetan radioimmunotherapy. J Clin Oncol. 2007;25(27):4285-92.
28. Granfeldt Ostgard LS, Medeiros BC, Sengelov H, Norgaard M, Andersen MK, Dufva IH, et al. Epidemiology and Clinical Significance of Secondary and Therapy-Related Acute Myeloid Leukemia: A National Population-Based Cohort Study. J Clin Oncol. 2015;33(31):3641-9.

29. Sill H, Olipitz W, Zebisch A, Schulz E, Wolfler A. Therapy-related myeloid neoplasms: pathobiology and clinical characteristics. Br J Pharmacol. 2011;162(4):792-805.
30. Furutani E, Shimamura A. Germline Genetic Predisposition to Hematologic Malignancy. J Clin Oncol. 2017;35(9):1018-28.
31. Wartiovaara-Kautto U, Hirvonen EAM, Pitkanen E, Heckman C, Saarela J, Kettunen K, et al. Germline alterations in a consecutive series of acute myeloid leukemia. Leukemia. 2018;32(10):2282-5.
32. Seiter K, Htun K, Baskind P, Liu Z. Acute myeloid leukemia in a father and son with a germline mutation of ASXL1. Biomark Res. 2018;6:7.
33. Li R, Sobreira N, Witmer PD, Pratz KW, Braunstein EM. Two novel germline DDX41 mutations in a family with inherited myelodysplasia/acute myeloid leukemia. Haematologica. 2016;101(6):e228-31.
34. Tawana K, Wang J, Renneville A, Bodor C, Hills R, Loveday C, et al. Disease evolution and outcomes in familial AML with germline CEBPA mutations. Blood. 2015;126(10):1214-23.
35. Gao J, Gentzler RD, Timms AE, Horwitz MS, Frankfurt O, Altman JK, et al. Heritable GATA2 mutations associated with familial AML-MDS: a case report and review of literature. J Hematol Oncol. 2014;7:36.
36. Ganly P, Walker LC, Morris CM. Familial mutations of the transcription factor RUNX1 (AML1, CBFA2) predispose to acute myeloid leukemia. Leuk Lymphoma. 2004;45(1):1-10.
37. Zebisch A, Lal R, Muller M, Lind K, Kashofer K, Girschikofsky M, et al. Acute myeloid leukemia with TP53 germ line mutations. Blood. 2016;128(18):2270-2.
38. Taub JW. Relationship of chromosome 21 and acute leukemia in children with Down syndrome. J Pediatr Hematol Oncol. 2001;23(3):175-8.
39. Zhang J, Nichols KE, Downing JR. Germline Mutations in Predisposition Genes in Pediatric Cancer. N Engl J Med. 2016;374(14):1391.
40. Yoshida K, Toki T, Okuno Y, Kanezaki R, Shiraishi Y, Sato-Otsubo A, et al. The landscape of somatic mutations in Down syndrome-related myeloid disorders. Nat Genet. 2013;45(11):1293-9.
41. Smith ML, Cavenagh JD, Lister TA, Fitzgibbon J. Mutation of CEBPA in familial acute myeloid leukemia. N Engl J Med. 2004;351(23):2403-7.
42. Mitelman F, Johansson B, Mertens F. The impact of translocations and gene fusions on cancer causation. Nat Rev Cancer. 2007;7(4):233-45.

43. Shlush LI, Zandi S, Mitchell A, Chen WC, Brandwein JM, Gupta V, et al. Identification of pre-leukaemic haematopoietic stem cells in acute leukaemia. Nature. 2014;506(7488):328-33.
44. Corces-Zimmerman MR, Hong WJ, Weissman IL, Medeiros BC, Majeti R. Preleukemic mutations in human acute myeloid leukemia affect epigenetic regulators and persist in remission. Proc Natl Acad Sci U S A. 2014;111(7):2548-53.
45. Jan M, Snyder TM, Corces-Zimmerman MR, Vyas P, Weissman IL, Quake SR, et al. Clonal evolution of preleukemic hematopoietic stem cells precedes human acute myeloid leukemia. Sci Transl Med. 2012;4(149):149ra18.
46. Pulikkan JA, Castilla LH. Preleukemia and Leukemia-Initiating Cell Activity in inv(16) Acute Myeloid Leukemia. Front Oncol. 2018;8:129.
47. Welch JS, Ley TJ, Link DC, Miller CA, Larson DE, Koboldt DC, et al. The origin and evolution of mutations in acute myeloid leukemia. Cell. 2012;150(2):264-78.
48. Mora-Jensen H, Jendholm J, Rapin N, Andersen MK, Roug AS, Bagger FO, et al. Cellular origin of prognostic chromosomal aberrations in AML patients. Leukemia. 2015;29(8):1785-9.
49. Hou HA, Kuo YY, Liu CY, Chou WC, Lee MC, Chen CY, et al. DNMT3A mutations in acute myeloid leukemia: stability during disease evolution and clinical implications. Blood. 2012;119(2):559-68.
50. Cloos J, Goemans BF, Hess CJ, van Oostveen JW, Waisfisz Q, Corthals S, et al. Stability and prognostic influence of FLT3 mutations in paired initial and relapsed AML samples. Leukemia. 2006;20(7):1217-20.
51. Riemke P, Czeh M, Fischer J, Walter C, Ghani S, Zepper M, et al. Myeloid leukemia with transdifferentiation plasticity developing from T-cell progenitors. EMBO J. 2016;35(22):2399-416.
52. Walter RB, Appelbaum FR, Estey EH, Bernstein ID. Acute myeloid leukemia stem cells and CD33-targeted immunotherapy. Blood. 2012;119(26):6198-208.
53. Essers MA, Trumpp A. Targeting leukemic stem cells by breaking their dormancy. Mol Oncol. 2010;4(5):443-50.
54. Krivtsov AV, Figueroa ME, Sinha AU, Stubbs MC, Feng Z, Valk PJ, et al. Cell of origin determines clinically relevant subtypes of MLL-rearranged AML. Leukemia. 2013;27(4):852-60.
55. George J, Uyar A, Young K, Kuffler L, Waldron-Francis K, Marquez E, et al. Leukaemia cell of origin identified by chromatin landscape of bulk tumour cells. Nat Commun. 2016;7:12166.
56. Plesa A, Dumontet C, Mattei E, Tagoug I, Hayette S, Sujobert P, et al. High frequency of CD34+CD38-/low immature leukemia cells is correlated with unfavorable prognosis in acute myeloid leukemia. World J Stem Cells. 2017;9(12):227-34.

57. McKerrell T, Park N, Moreno T, Grove CS, Ponstingl H, Stephens J, et al. Leukemia-associated somatic mutations drive distinct patterns of age-related clonal hemopoiesis. Cell Rep. 2015;10(8):1239-45.
58. Eisfeld AK, Kohlschmidt J, Mrozek K, Blachly JS, Walker CJ, Nicolet D, et al. Mutation patterns identify adult patients with de novo acute myeloid leukemia aged 60 years or older who respond favorably to standard chemotherapy: an analysis of Alliance studies. Leukemia. 2018;32(6):1338-48.
59. Finnish Cancer Registry. Cancer Statistics 2018 [cited 2018 Nov 13]. Available from: https://cancerregistry.fi/statistics/cancer-statistics/.
60. National Cancer Institute. Seer Cancer Statistics Fact sheets: Acute Myeloid Leukemia: National Cancer Institute: Bethesda, MD, USA; 2018 [Available from: https://seer.cancer.gov/statfacts/html/amyl.html.
61. Cancer Research UK. Acute myeloid leukaemia (AML) incidence statistics 2018 [Available from: https://www.cancerresearchuk.org/health-professional/cancer-statistics/statistics-by-cancer-type/leukaemia-aml/incidence.
62. Siegel RL, Miller KD, Jemal A. Cancer statistics, 2018. CA Cancer J Clin. 2018;68(1):7-30.
63. Dohner H, Estey E, Grimwade D, Amadori S, Appelbaum FR, Buchner T, et al. Diagnosis and management of AML in adults: 2017 ELN recommendations from an international expert panel. Blood. 2017;129(4):424-47.
64. Dohner H, Estey EH, Amadori S, Appelbaum FR, Buchner T, Burnett AK, et al. Diagnosis and management of acute myeloid leukemia in adults: recommendations from an international expert panel, on behalf of the European LeukemiaNet. Blood. 2010;115(3):453-74.
65. Arber DA, Orazi A, Hasserjian R, Thiele J, Borowitz MJ, Le Beau MM, et al. The 2016 revision to the World Health Organization classification of myeloid neoplasms and acute leukemia. Blood. 2016;127(20):2391-405.
66. Churpek JE, Pyrtel K, Kanchi KL, Shao J, Koboldt D, Miller CA, et al. Genomic analysis of germ line and somatic variants in familial myelodysplasia/acute myeloid leukemia. Blood. 2015;126(22):2484-90.
67. Bene MC, Nebe T, Bettelheim P, Buldini B, Bumbea H, Kern W, et al. Immunophenotyping of acute leukemia and lymphoproliferative disorders: a consensus proposal of the European LeukemiaNet Work Package 10. Leukemia. 2011;25(4):567-74.
68. Bacher U, Shumilov E, Flach J, Porret N, Joncourt R, Wiedemann G, et al. Challenges in the introduction of next-generation sequencing (NGS) for diagnostics of myeloid malignancies into clinical routine use. Blood Cancer J. 2018;8(11):113.
69. Bennett JM, Catovsky D, Daniel MT, Flandrin G, Galton DA, Gralnick HR, et al. Proposals for the classification of the acute leukaemias.

French-American-British (FAB) co-operative group. Br J Haematol. 1976;33(4):451-8.
70. Bloomfield CD, Brunning RD. FAB M7: acute megakaryoblastic leukemia--beyond morphology. Ann Intern Med. 1985;103(3):450-2.
71. Bennett JM, Catovsky D, Daniel MT, Flandrin G, Galton DA, Gralnick HR, et al. Proposal for the recognition of minimally differentiated acute myeloid leukaemia (AML-MO). Br J Haematol. 1991;78(3):325-9.
72. Jaffe ES HN, Stein H, Vardiman JW. Pathology and Genetics of Tumours of
Haematopoietic and Lymphoid Tissues.
. IARC Press, Lyon 2001.
73. Swerdlow SH CE, Harris NL, et al. WHO Classification of Tumours of Haematopoietic and Lymphoid Tissues. Lyon, France: IARC; 2008. 2008.
74. S.H. Swerdlow EC, N.L. Harris, E.S. Jaffe, S.A. Pileri, H. Stein, J. Thiele, D. Arber, R. Hasserjian, M. Le Beau. WHO Classification of Tumours of Haematopoietic and Lymphoid Tissues (Revised 4th Ed, Vol 2). Lyon, France: IARC. 2017.
75. Liersch R, Muller-Tidow C, Berdel WE, Krug U. Prognostic factors for acute myeloid leukaemia in adults--biological significance and clinical use. Br J Haematol. 2014;165(1):17-38.
76. Appelbaum FR, Gundacker H, Head DR, Slovak ML, Willman CL, Godwin JE, et al. Age and acute myeloid leukemia. Blood. 2006;107(9):3481-5.
77. McCurdy SR, Levis MJ. Emerging molecular predictive and prognostic factors in acute myeloid leukemia. Leuk Lymphoma. 2018;59(9):2021-39.
78. National Comprehensive Cancer Network (NCCN). NCCN clinical practice guidelines in oncology. Acute myeloid leukemia version 1. 2018 [Available from: https://www.nccn.org/professionals/physician_gls/pdf/aml.pdf.
79. Patel JP, Gonen M, Figueroa ME, Fernandez H, Sun Z, Racevskis J, et al. Prognostic relevance of integrated genetic profiling in acute myeloid leukemia. N Engl J Med. 2012;366(12):1079-89.
80. FDA. [Available from: http://www.fda.gov/Drugs/InformationOnDrugs/ApprovedDrugs/ucm614128.thm.
81. Stein EM, DiNardo CD, Pollyea DA, Fathi AT, Roboz GJ, Altman JK, et al. Enasidenib in mutant IDH2 relapsed or refractory acute myeloid leukemia. Blood. 2017;130(6):722-31.
82. Juliusson G, Antunovic P, Derolf A, Lehmann S, Mollgard L, Stockelberg D, et al. Age and acute myeloid leukemia: real world data on decision to treat and outcomes from the Swedish Acute Leukemia Registry. Blood. 2009;113(18):4179-87.

83. Wang ZY, Chen Z. Acute promyelocytic leukemia: from highly fatal to highly curable. Blood. 2008;111(5):2505-15.
84. Lancet JE, Uy GL, Cortes JE, Newell LF, Lin TL, Ritchie EK, et al. CPX-351 (cytarabine and daunorubicin) Liposome for Injection Versus Conventional Cytarabine Plus Daunorubicin in Older Patients With Newly Diagnosed Secondary Acute Myeloid Leukemia. J Clin Oncol. 2018;36(26):2684-92.
85. Stone RM, Mandrekar SJ, Sanford BL, Laumann K, Geyer S, Bloomfield CD, et al. Midostaurin plus Chemotherapy for Acute Myeloid Leukemia with a FLT3 Mutation. N Engl J Med. 2017;377(5):454-64.
86. Stone RM, Larson RA, Dohner H. Midostaurin in FLT3-Mutated Acute Myeloid Leukemia. N Engl J Med. 2017;377(19):1903.
87. Gottardi M, Mosna F, de Angeli S, Papayannidis C, Candoni A, Clavio M, et al. Clinical and experimental efficacy of gemtuzumab ozogamicin in core binding factor acute myeloid leukemia. Hematol Rep. 2017;9(3):7029.
88. Tack DK, Letendre L, Kamath PS, Tefferi A. Development of hepatic veno-occlusive disease after Mylotarg infusion for relapsed acute myeloid leukemia. Bone Marrow Transplant. 2001;28(9):895-7.
89. Peccatori J, Ciceri F. Allogeneic stem cell transplantation for acute myeloid leukemia. Haematologica. 2010;95(6):857-9.
90. Salvatore D, Labopin M, Ruggeri A, Battipaglia G, Ghavamzadeh A, Ciceri F, et al. Outcomes of hematopoietic stem cell transplantation from unmanipulated haploidentical versus matched sibling donor in patients with acute myeloid leukemia in first complete remission with intermediate or high-risk cytogenetics: a study from the Acute Leukemia Working Party of the European Society for Blood and Marrow Transplantation. Haematologica. 2018;103(8):1317-28.
91. Podoltsev NA, Stahl M, Zeidan AM, Gore SD. Selecting initial treatment of acute myeloid leukaemia in older adults. Blood Rev. 2017;31(2):43-62.
92. Walter RB, Estey EH. Management of older or unfit patients with acute myeloid leukemia. Leukemia. 2015;29(4):770-5.
93. FDA. [Available from: http://www.fda.gov/Drugs/InformationOnDrugs/ApprovedDrugs/ucm626494.htm.
94. Andrew Wei SAS, Gail J. Roboz, Jing-Zhou Hou, Walter Fiedler, Tara L. Lin, Giovanni Martinelli, Roland B. Walter, Anoop Enjeti, et al. Safety and Efficacy of Venetoclax Plus Low-Dose Cytarabine in Treatment-Naive Patients Aged ≥65 Years with Acute Myeloid Leukemia. Blood; 2016.
95. DiNardo CD, Pratz K, Pullarkat V, Jonas BA, Arellano M, Becker PS, et al. Venetoclax combined with decitabine or azacitidine in treatment-naive, elderly patients with acute myeloid leukemia. Blood. 2019;133(1):7-17.

96. Schlenk RF, Frech P, Weber D, Brossart P, Horst HA, Kraemer D, et al. Impact of pretreatment characteristics and salvage strategy on outcome in patients with relapsed acute myeloid leukemia. Leukemia. 2017;31(5):1217-20.
97. Schlenk RF, Muller-Tidow C, Benner A, Kieser M. Relapsed/refractory acute myeloid leukemia: any progress? Curr Opin Oncol. 2017;29(6):467-73.
98. Kayser S, Levis MJ. Advances in targeted therapy for acute myeloid leukaemia. Br J Haematol. 2018;180(4):484-500.
99. Wang ES TM, Stone RM, et al. Low relapse rate in younger patients≤ 60 years old with newly diagnosed flt3-mutated acute myeloid leukemia (aml) treated with crenolanib and cytarabine/anthracycline chemotherapy. Am Soc Hematology: Blood; 2017.
100. Pratz KW, Sato T, Murphy KM, Stine A, Rajkhowa T, Levis M. FLT3-mutant allelic burden and clinical status are predictive of response to FLT3 inhibitors in AML. Blood. 2010;115(7):1425-32.
101. Pratz KW, Levis M. How I treat FLT3-mutated AML. Blood. 2017;129(5):565-71.
102. Chaturvedi A, Herbst L, Pusch S, Klett L, Goparaju R, Stichel D, et al. Pan-mutant-IDH1 inhibitor BAY1436032 is highly effective against human IDH1 mutant acute myeloid leukemia in vivo. Leukemia. 2017;31(10):2020-8.
103. Blum S, Martins F, Lubbert M. Immunotherapy in adult acute leukemia. Leuk Res. 2017;60:63-73.
104. Pollyea DA, Jordan CT. Therapeutic targeting of acute myeloid leukemia stem cells. Blood. 2017;129(12):1627-35.
105. Tyner JW, Tognon CE, Bottomly D, Wilmot B, Kurtz SE, Savage SL, et al. Functional genomic landscape of acute myeloid leukaemia. Nature. 2018;562(7728):526-31.
106. Kabachinski G, Schwartz TU. The nuclear pore complex--structure and function at a glance. J Cell Sci. 2015;128(3):423-9.
107. Borrow J, Shearman AM, Stanton VP, Jr., Becher R, Collins T, Williams AJ, et al. The t(7;11)(p15;p15) translocation in acute myeloid leukaemia fuses the genes for nucleoporin NUP98 and class I homeoprotein HOXA9. Nat Genet. 1996;12(2):159-67.
108. Nakamura T, Largaespada DA, Lee MP, Johnson LA, Ohyashiki K, Toyama K, et al. Fusion of the nucleoporin gene NUP98 to HOXA9 by the chromosome translocation t(7;11)(p15;p15) in human myeloid leukaemia. Nat Genet. 1996;12(2):154-8.
109. Gough S, Slape C, Aplan P. NUP98 gene fusions and hematological malignancies: common themes and new biologic insights. Blood. 2011;118(24):6247-57.
110. Saw J, Curtis DJ, Hussey DJ, Dobrovic A, Aplan PD, Slape CI. The fusion partner specifies the oncogenic potential of NUP98 fusion proteins. Leuk Res. 2013;37(12):1668-73.

111. Soler G, Kaltenbach S, Dobbelstein S, Broccardo C, Radford I, Mozziconacci MJ, et al. Identification of GSX2 and AF10 as NUP98 partner genes in myeloid malignancies. Blood Cancer J. 2013;3:e124.
112. Roussy M, Bilodeau M, Jouan L, Tibout P, Laramee L, Lemyre E, et al. NUP98-BPTF gene fusion identified in primary refractory acute megakaryoblastic leukemia of infancy. Genes Chromosomes Cancer. 2018;57(6):311-9.
113. Thibodeau ML, Steinraths M, Brown L, Zong Z, Shomer N, Taubert S, et al. Genomic and Cytogenetic Characterization of a Balanced Translocation Disrupting NUP98. Cytogenet Genome Res. 2017;152(3):117-21.
114. Ahuja HG, Hong J, Aplan PD, Tcheurekdjian L, Forman SJ, Slovak ML. t(9;11)(p22;p15) in acute myeloid leukemia results in a fusion between NUP98 and the gene encoding transcriptional coactivators p52 and p75-lens epithelium-derived growth factor (LEDGF). Cancer Res. 2000;60(22):6227-9.
115. Raza-Egilmez SZ, Jani-Sait SN, Grossi M, Higgins MJ, Shows TB, Aplan PD. NUP98-HOXD13 gene fusion in therapy-related acute myelogenous leukemia. Cancer Res. 1998;58(19):4269-73.
116. Hollink IH, van den Heuvel-Eibrink MM, Arentsen-Peters ST, Pratcorona M, Abbas S, Kuipers JE, et al. NUP98/NSD1 characterizes a novel poor prognostic group in acute myeloid leukemia with a distinct HOX gene expression pattern. Blood. 2011;118(13):3645-56.
117. Romana SP, Radford-Weiss I, Ben Abdelali R, Schluth C, Petit A, Dastugue N, et al. NUP98 rearrangements in hematopoietic malignancies: a study of the Groupe Francophone de Cytogenetique Hematologique. Leukemia. 2006;20(4):696-706.
118. Jaju RJ, Haas OA, Neat M, Harbott J, Saha V, Boultwood J, et al. A new recurrent translocation, t(5;11)(q35;p15.5), associated with del(5q) in childhood acute myeloid leukemia. The UK Cancer Cytogenetics Group (UKCCG). Blood. 1999;94(2):773-80.
119. Jaju RJ, Fidler C, Haas OA, Strickson AJ, Watkins F, Clark K, et al. A novel gene, NSD1, is fused to NUP98 in the t(5;11)(q35;p15.5) in de novo childhood acute myeloid leukemia. Blood. 2001;98(4):1264-7.
120. Ostronoff F, Othus M, Gerbing RB, Loken MR, Raimondi SC, Hirsch BA, et al. NUP98/NSD1 and FLT3/ITD coexpression is more prevalent in younger AML patients and leads to induction failure: a COG and SWOG report. Blood. 2014;124(15):2400-7.
121. Thol F, Kolking B, Hollink IH, Damm F, van den Heuvel-Eibrink MM, Michel Zwaan C, et al. Analysis of NUP98/NSD1 translocations in adult AML and MDS patients. Leukemia. 2013;27(3):750-4.
122. Akiki S, Dyer SA, Grimwade D, Ivey A, Abou-Zeid N, Borrow J, et al. NUP98-NSD1 fusion in association with FLT3-ITD mutation identifies a prognostically relevant subgroup of pediatric acute

myeloid leukemia patients suitable for monitoring by real time quantitative PCR. Genes Chromosomes Cancer. 2013;52(11):1053-64.
123. Cerveira N, Correia C, Doria S, Bizarro S, Rocha P, Gomes P, et al. Frequency of NUP98-NSD1 fusion transcript in childhood acute myeloid leukaemia. Leukemia. 2003;17(11):2244-7.
124. Shiba N, Ichikawa H, Taki T, Park MJ, Jo A, Mitani S, et al. NUP98-NSD1 gene fusion and its related gene expression signature are strongly associated with a poor prognosis in pediatric acute myeloid leukemia. Genes Chromosomes Cancer. 2013;52(7):683-93.
125. Nebral K, Konig M, Schmidt HH, Lutz D, Sperr WR, Kalwak K, et al. Screening for NUP98 rearrangements in hematopoietic malignancies by fluorescence in situ hybridization. Haematologica. 2005;90(6):746-52.
126. Struski S, Lagarde S, Bories P, Puiseux C, Prade N, Cuccuini W, et al. NUP98 is rearranged in 3.8% of pediatric AML forming a clinical and molecular homogenous group with a poor prognosis. Leukemia. 2017;31(3):565-72.
127. Fasan A, Haferlach C, Alpermann T, Kern W, Haferlach T, Schnittger S. A rare but specific subset of adult AML patients can be defined by the cytogenetically cryptic NUP98-NSD1 fusion gene. Leukemia. 2013;27(1):245-8.
128. Lavallee VP, Lemieux S, Boucher G, Gendron P, Boivin I, Girard S, et al. Identification of MYC mutations in acute myeloid leukemias with NUP98-NSD1 translocations. Leukemia. 2016;30(7):1621-4.
129. Wang GG, Cai L, Pasillas MP, Kamps MP. NUP98-NSD1 links H3K36 methylation to Hox-A gene activation and leukaemogenesis. Nat Cell Biol. 2007;9(7):804-12.
130. Fahrenkrog B, Martinelli V, Nilles N, Fruhmann G, Chatel G, Juge S, et al. Expression of Leukemia-Associated Nup98 Fusion Proteins Generates an Aberrant Nuclear Envelope Phenotype. PLoS One. 2016;11(3):e0152321.
131. Xu H, Valerio DG, Eisold ME, Sinha A, Koche RP, Hu W, et al. NUP98 Fusion Proteins Interact with the NSL and MLL1 Complexes to Drive Leukemogenesis. Cancer Cell. 2016;30(6):863-78.
132. Oka M, Mura S, Yamada K, Sangel P, Hirata S, Maehara K, et al. Chromatin-prebound Crm1 recruits Nup98-HoxA9 fusion to induce aberrant expression of Hox cluster genes. Elife. 2016;5:e09540.
133. Franks TM, McCloskey A, Shokirev MN, Benner C, Rathore A, Hetzer MW. Nup98 recruits the Wdr82-Set1A/COMPASS complex to promoters to regulate H3K4 trimethylation in hematopoietic progenitor cells. Genes Dev. 2017;31(22):2222-34.
134. Deshpande AJ, Deshpande A, Sinha AU, Chen L, Chang J, Cihan A, et al. AF10 regulates progressive H3K79 methylation and HOX gene expression in diverse AML subtypes. Cancer Cell. 2014;26(6):896-908.

135. Hussey DJ, Dobrovic A. Recurrent coiled-coil motifs in NUP98 fusion partners provide a clue to leukemogenesis. Blood. 2002;99(3):1097-8.
136. Cui J, Xie J, Qin L, Chen S, Zhao Y, Wu D. A unique acute myeloid leukemia patient with cryptic NUP98-NSD1 gene and ASXL1 mutation. Leuk Lymphoma. 2016;57(1):196-8.
137. Bisio V, Zampini M, Tregnago C, Manara E, Salsi V, Di Meglio A, et al. NUP98-fusion transcripts characterize different biological entities within acute myeloid leukemia: a report from the AIEOP-AML group. Leukemia. 2017;31(4):974-7.
138. Crescenzi B, Nofrini V, Barba G, Matteucci C, Di Giacomo D, Gorello P, et al. NUP98/11p15 translocations affect CD34+ cells in myeloid and T lymphoid leukemias. Leuk Res. 2015;39(7):769-72.
139. Panarello C, Rosanda C, Morerio C. Cryptic translocation t(5;11)(q35;p15.5) with involvement of the NSD1 and NUP98 genes without 5q deletion in childhood acute myeloid leukemia. Genes Chromosomes Cancer. 2002;35(3):277-81.
140. Kivioja JL, Lopez Marti JM, Kumar A, Kontro M, Edgren H, Parsons A, et al. Chimeric NUP98-NSD1 transcripts from the cryptic t(5;11)(q35.2;p15.4) in adult de novo acute myeloid leukemia. Leuk Lymphoma. 2018;59(3):725-32.
141. Petit A, Radford I, Waill MC, Romana S, Berger R. NUP98-NSD1 fusion by insertion in acute myeloblastic leukemia. Cancer Genet Cytogenet. 2008;180(1):43-6.
142. Drenberg CD, Buelow DR, Pounds SB, Wang YD, Finkelstein D, Rahija RJ, et al. Transcriptome profiling of patient derived xenograft models established from pediatric acute myeloid leukemia patients confirm maintenance of FLT3-ITD mutation. Leuk Lymphoma. 2017;58(1):247-50.
143. Shiba N, Ohki K, Kobayashi T, Hara Y, Yamato G, Tanoshima R, et al. High PRDM16 expression identifies a prognostic subgroup of pediatric acute myeloid leukaemia correlated to FLT3-ITD, KMT2A-PTD, and NUP98-NSD1: the results of the Japanese Paediatric Leukaemia/Lymphoma Study Group AML-05 trial. Br J Haematol. 2016;172(4):581-91.
144. Shimada A, Iijima-Yamashita Y, Tawa A, Tomizawa D, Yamada M, Norio S, et al. Risk-stratified therapy for children with FLT3-ITD-positive acute myeloid leukemia: results from the JPLSG AML-05 study. Int J Hematol. 2018;107(5):586-95.
145. Bolouri H, Farrar JE, Triche T, Jr., Ries RE, Lim EL, Alonzo TA, et al. The molecular landscape of pediatric acute myeloid leukemia reveals recurrent structural alterations and age-specific mutational interactions. Nat Med. 2018;24(1):103-12.
146. Thanasopoulou A, Tzankov A, Schwaller J. Potent co-operation between the NUP98-NSD1 fusion and the FLT3-ITD mutation in acute myeloid leukemia induction. Haematologica. 2014;99(9):1465-71.

147. Zhang JH, Chung TD, Oldenburg KR. A Simple Statistical Parameter for Use in Evaluation and Validation of High Throughput Screening Assays. J Biomol Screen. 1999;4(2):67-73.
148. Yadav B, Pemovska T, Szwajda A, Kulesskiy E, Kontro M, Karjalainen R, et al. Quantitative scoring of differential drug sensitivity for individually optimized anticancer therapies. Sci Rep. 2014;4:5193.
149. Pemovska T, Kontro M, Yadav B, Edgren H, Eldfors S, Szwajda A, et al. Individualized systems medicine strategy to tailor treatments for patients with chemorefractory acute myeloid leukemia. Cancer discovery. 2013;3(12):1416-29.
150. Yadav B, Wennerberg K, Aittokallio T, Tang J. Searching for Drug Synergy in Complex Dose-Response Landscapes Using an Interaction Potency Model. Comput Struct Biotechnol J. 2015;13:504-13.
151. Ianevski A, He L, Aittokallio T, Tang J. SynergyFinder: a web application for analyzing drug combination dose-response matrix data. Bioinformatics. 2017;33(15):2413-5.
152. Trapnell C, Pachter L, Salzberg SL. TopHat: discovering splice junctions with RNA-Seq. Bioinformatics. 2009;25(9):1105-11.
153. Nicorici D, Satalan M, Edgren H, Kangaspeska S, Murumagi A, Kallioniemi O, et al. FusionCatcher - a tool for finding somatic fusion genes in paired-end RNA-sequencing data. bioRxiv. 2014.
154. Robinson JT, Thorvaldsdottir H, Winckler W, Guttman M, Lander ES, Getz G, et al. Integrative genomics viewer. Nat Biotechnol. 2011;29(1):24-6.
155. Li H, Handsaker B, Wysoker A, Fennell T, Ruan J, Homer N, et al. The Sequence Alignment/Map format and SAMtools. Bioinformatics. 2009;25(16):2078-9.
156. Dobin A, Davis CA, Schlesinger F, Drenkow J, Zaleski C, Jha S, et al. STAR: ultrafast universal RNA-seq aligner. Bioinformatics. 2013;29(1):15-21.
157. Robinson MD, Oshlack A. A scaling normalization method for differential expression analysis of RNA-seq data. Genome Biol. 2010;11(3):R25.
158. Edgren H, Murumagi A, Kangaspeska S, Nicorici D, Hongisto V, Kleivi K, et al. Identification of fusion genes in breast cancer by paired-end RNA-sequencing. Genome Biol. 2011;12(1):R6.
159. Eldfors S, Kuusanmaki H, Kontro M, Majumder MM, Parsons A, Edgren H, et al. Idelalisib sensitivity and mechanisms of disease progression in relapsed TCF3-PBX1 acute lymphoblastic leukemia. Leukemia. 2017;31(1):51-7.
160. Zwaan CM, Meshinchi S, Radich JP, Veerman AJ, Huismans DR, Munske L, et al. FLT3 internal tandem duplication in 234 children with acute myeloid leukemia: prognostic significance and relation to cellular drug resistance. Blood. 2003;102(7):2387-94.
161. Hayakawa F, Towatari M, Kiyoi H, Tanimoto M, Kitamura T, Saito H, et al. Tandem-duplicated Flt3 constitutively activates STAT5

and MAP kinase and introduces autonomous cell growth in IL-3-dependent cell lines. Oncogene. 2000;19(5):624-31.
162. Shi J, Shao ZH, Liu H, Bai J, Cao YR, He GS, et al. Transformation of myelodysplastic syndromes into acute myeloid leukemias. Chin Med J (Engl). 2004;117(7):963-7.
163. Audemard É, Gendron P, Lavallée V-P, Hébert J, Sauvageau G, Lemieux S. Target variant detection in leukemia using unaligned RNA-Seq reads. bioRxiv. 2018:295808.
164. Adler R, Viehmann S, Kuhlisch E, Martiniak Y, Rottgers S, Harbott J, et al. Correlation of BCR/ABL transcript variants with patients' characteristics in childhood chronic myeloid leukaemia. Eur J Haematol. 2009;82(2):112-8.
165. Andrikovics H, Nahajevszky S, Szilvasi A, Bors A, Adam E, Kozma A, et al. First and second line imatinib treatment in chronic myelogenous leukemia patients expressing rare e1a2 or e19a2 BCR-ABL transcripts. Hematol Oncol. 2007;25(3):143-7.
166. Lin HX, Sjaarda J, Dyck J, Stringer R, Hillis C, Harvey M, et al. Gender and BCR-ABL transcript type are correlated with molecular response to imatinib treatment in patients with chronic myeloid leukemia. Eur J Haematol. 2016;96(4):360-6.
167. Paschka P, Schlenk RF, Weber D, Benner A, Bullinger L, Heuser M, et al. Adding dasatinib to intensive treatment in core-binding factor acute myeloid leukemia-results of the AMLSG 11-08 trial. Leukemia. 2018;32(7):1621-30.
168. Marhall A, Kazi JU, Ronnstrand L. The Src family kinase LCK cooperates with oncogenic FLT3/ITD in cellular transformation. Sci Rep. 2017;7(1):13734.
169. Rayasam GV, Wendling O, Angrand PO, Mark M, Niederreither K, Song L, et al. NSD1 is essential for early post-implantation development and has a catalytically active SET domain. EMBO J. 2003;22(12):3153-63.
170. Benito JM, Godfrey L, Kojima K, Hogdal L, Wunderlich M, Geng H, et al. MLL-Rearranged Acute Lymphoblastic Leukemias Activate BCL-2 through H3K79 Methylation and Are Sensitive to the BCL-2-Specific Antagonist ABT-199. Cell Rep. 2015;13(12):2715-27.
171. Lu T, Jackson MW, Wang B, Yang M, Chance MR, Miyagi M, et al. Regulation of NF-kappaB by NSD1/FBXL11-dependent reversible lysine methylation of p65. Proc Natl Acad Sci U S A. 2010;107(1):46-51.
172. Wang CY, Guttridge DC, Mayo MW, Baldwin AS, Jr. NF-kappaB induces expression of the Bcl-2 homologue A1/Bfl-1 to preferentially suppress chemotherapy-induced apoptosis. Mol Cell Biol. 1999;19(9):5923-9.
173. Kontro M, Kumar A, Majumder MM, Eldfors S, Parsons A, Pemovska T, et al. HOX gene expression predicts response to BCL-2 inhibition in acute myeloid leukemia. Leukemia. 2017;31(2):301-9.

174. Morrison DJ, English MA, Licht JD. WT1 induces apoptosis through transcriptional regulation of the proapoptotic Bcl-2 family member Bak. Cancer Res. 2005;65(18):8174-82.
175. Kasper LH, Brindle PK, Schnabel CA, Pritchard CE, Cleary ML, van Deursen JM. CREB binding protein interacts with nucleoporin-specific FG repeats that activate transcription and mediate NUP98-HOXA9 oncogenicity. Mol Cell Biol. 1999;19(1):764-76.
176. Greenblatt S, Li L, Slape C, Nguyen B, Novak R, Duffield A, et al. Knock-in of a FLT3/ITD mutation cooperates with a NUP98-HOXD13 fusion to generate acute myeloid leukemia in a mouse model. Blood. 2012;119(12):2883-94.
177. Stubbs MC, Kim YM, Krivtsov AV, Wright RD, Feng Z, Agarwal J, et al. MLL-AF9 and FLT3 cooperation in acute myelogenous leukemia: development of a model for rapid therapeutic assessment. Leukemia. 2008;22(1):66-77.
178. Blo M, Micklem DR, Lorens JB. Enhanced gene expression from retroviral vectors. BMC Biotechnol. 2008;8:19.